DALTON
FULL PAPER

# *tert*-Butyl compounds of gallium

**Andrea Keys,[a] Thomas J. Barbarich,[a] Simon G. Bott *[b] and Andrew R. Barron *[a]**

[a] *Department of Chemistry, Rice University, Houston, Texas 77005, USA*
[b] *Department of Chemistry, University of Houston, Houston, Texas 77204, USA*

***Received 30th June 1999, Accepted 16th December 1999***

The *tert*-butyl substituted compounds of gallium have been synthesized and characterized: $[(^tBu)_2Ga\{\mu\text{-}OCH(CF_3)_2\}]_2$ (**1**), $[(^tBu)_2Ga(\mu\text{-}O_2CEt)]_2$ (**2**), $[(^tBu)_2Ga(\mu\text{-}O_2CCF_3)]_2$ (**3**), $[(^tBu)_2Ga\{\mu\text{-}OC(Ph)N(H)\}]_2$ (**4**), $[(^tBu)_2Ga\{\mu\text{-}OC(Me)NPh\}]_2$ (**5**), $(^tBu)_3Ga[OC(Ph)NMe_2]$ (**6**), $(^tBu)_3Ga[OP(Ph)_2NH(^nPr)]$ (**7**), $(^tBu)_2Ga[ON(H)C(O)Ph]$ (**8**), $[(^tBu)_2Ga\{\mu\text{-}O_2S(CF_3)O\}]_2$ (**9**), $(^tBu)_2Ga(\mu\text{-}Cl)_2Li(HO^iPr)_2$ (**10**), and $[Li(HO^iPr)_4][(^tBu)_2GaCl_2]$ (**11**). X-Ray crystallographic characterization was obtained for compounds **1**–**6** and **8**–**11**. Compounds **10** and **11** exhibit three-dimensional hydrogen bonded networks in which augmentation of the O–H · · · Cl hydrogen bond is proposed to be due to the increased acidity of alcohols bonded to the Lewis acidic lithium ions. A discussion of the dependence of the puckering of the chair-like conformation in eight-membered cyclic compounds of the Group 13 metals is presented.

## Introduction

During the 1990's much of the research in our group has involved the *tert*-butyl derivatives of the Group 13 metals aluminium, gallium and indium.[1] The rationale for employing the *tert*-butyl group is multiple: first, the steric bulk as measured by the Tolman cone angle ($\theta = 126°$)[2] is large enough to allow isolation, but not sufficient to preclude formation of analogs of sterically less demanding alkyl groups. Second, the lack of stable *tert*-butyl bridges between two Group 13 metals, and hence high activation barrier to alkyl exchange, allows for isolation of species that would be fluxional (or in exchange equilibria) with primary or secondary alkyl groups.[3,4] Third, the majority of *tert*-butyl compounds of the Group 13 metals are solids and thus amenable to X-ray crystallographic characterization without significant disorder of the substituents.[5] Finally, while the NMR spectra of *tert*-butyl derivatives are relatively simple and lack any coupling or stereochemical information, the chemical shift of the $C(CH_3)_3$ protons are observed over a wide range ($\delta = 0.85$–$1.60$) and are highly indicative of the chemical environment.[6,7] All these factors have enabled us to prepare and structurally characterize a wide range of new compound types as well as understand the structure of previously complex systems. As part of our studies into the chemistry of gallium, we have structurally characterized di-*tert*-butyl derivatives of a wide range of ligands. These results are brought together herein and discussed within the context of our previous body of work. A summary of the results is given in Scheme 1.

## Results and discussion

### Alkoxide

Reaction of $Ga(^tBu)_3$ with one equivalent of $HOCH(CF_3)_2$ yields the expected alkoxide compound, $[(^tBu)_2Ga\{\mu\text{-}OCH(CF_3)_2\}]_2$ (**1**), in modest yield. Only a single type of both *tert*-butyl and $OCH(CF_3)_2$ ligands is observed in the $^1H$, $^{19}F$, and $^{13}C$ NMR spectra. The $^{13}C$ NMR spectrum shows the expected quartet absorption for $CF_3$ [$\delta = 123.5$; $J(C–F) = 284$ Hz] and septet for $C(CF_3)_2$ [$\delta = 74.2$; $J^2(C–F) = 31.8$ Hz].[8] Thus, the $^1H$, $^{13}C$ and $^{19}F$ NMR spectra are consistent with the formulation, while the mass spectrum indicates a dimeric structure, see Experimental section. The expected alkoxide bridged structure is confirmed by X-ray crystallography.

The molecular structure of compound **1** is shown in Fig. 1. Due to severe problems with the refinement (see Experimental section) only general comments may be made about the structure, however, the bond distances and angles are within expected ranges.[9] Despite the poor quality of the structure, one interesting feature is the apparent asymmetry of the alkoxide groups with respect to the O(1) · · · O(1′) vector, see Fig. 1. The significant distortion about oxygen [$\Delta(C–O–Ga) = 34°$] is best explained from a consideration of the space filling representation shown in Fig. 2 and the inter-ligand F · · · H–C distances. There are two sets of two close F · · · methyl distances, *i.e.*, F(31) · · · C(24) = 3.0 Å; F(33) · · · C(14) = 2.9 Å and F(31) · · · H(24C) = 2.2 Å; F(33) · · · H(14A) = 2.0 Å. These distances are significantly shorter than the sum of the van der Waals' radii [$\Sigma(F,Me) = 3.35$ Å, $\Sigma(F,H) = 2.55$ Å].[10] Furthermore, these distances are comparable to known C–F · · · H–C hydrogen bonding interactions,[11] however, they are undoubtedly purely steric in origin in the present case. As may be seen from Fig. 2, the $OCH(CF_3)_2$ ligand is wedged between the gallium *tert*-butyl groups forcing the close F · · · methyl distances.

We have previously reported[12] that for di-*tert*-butylgallium alkoxides the inter dimer Ga · · · Ga distance may readily act as a measure of the dominance of different packing forces. Thus, where the packing of the organometallic core is dominant, the Ga · · · Ga distance is relatively insensitive to the identity of R. Alternatively, when the packing of $[(Bu^t)_2Ga(\mu\text{-}OR)]_2$ is controlled by the hydrocarbon groups, R, the Ga · · · Ga distance varies systematically with increased chain length *n*. From a plot of Ga · · · Ga distance *versus n* the length of the alkoxide substituent R [$R = (CH_2)_nH$], see Fig. 3, we found that for chains shorter than $n = 6$, *i.e.*, Me to $n\text{-}C_5H_{11}$, there is little change in the Ga · · · Ga inter-dimer distance (8.805–8.956 Å). Even the sterically more demanding substituents (*e.g.*, *tert*-butyl) if included, show little deviation from the trend. In contrast, there is a large increase in the Ga · · · Ga distance when *n* is greater than 5, *i.e.*, hexyl, suggesting that amphiphilic interactions dominate the crystal packing forces for *n*-hexyl and longer hydrocarbon chains. If compound **1** is added to Fig. 3 as $n = 3$, it does not deviate from the expected trend.

DOI: 10.1039/a905281j

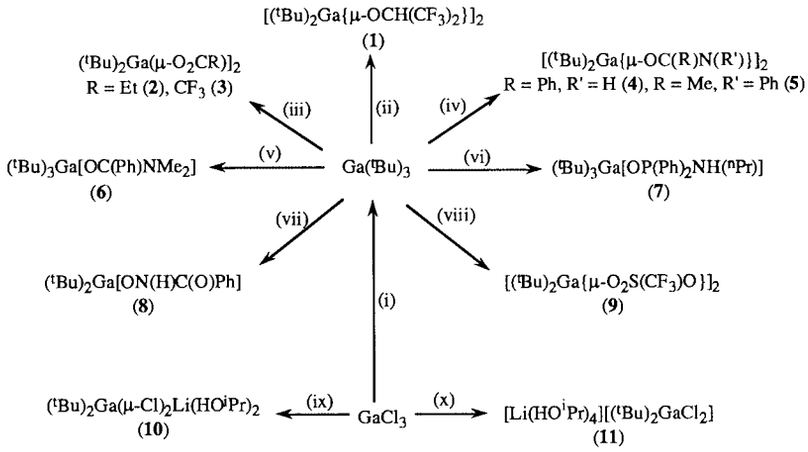


**Scheme 1** (i) $^{t}$BuLi, hexane. (ii) $HOCH(CF_3)_2$, hexane, −78 °C. (iii) $RCO_2H$, hexane, −78 °C. (iv) OC(R)NR′H, hexane or toluene, reflux. (v) $PhC(O)NMe_2$, hexane, −78 °C. (vi) $Ph_2P(O)NH(^{n}Pr)$, toluene, −78 °C. (vii) HON(H)C(O)Ph, hexane, −78 °C. (viii) $CF_3SO_3H$, hexane. (ix) $^{t}$BuLi, $Li(S_2CN^{i}Pr_2)$, hexane–$Et_2O$, −78 °C, $^{i}$PrOH. (x) $^{t}$BuLi, $Et_2O$, −78 °C, $^{i}$PrOH (excess).

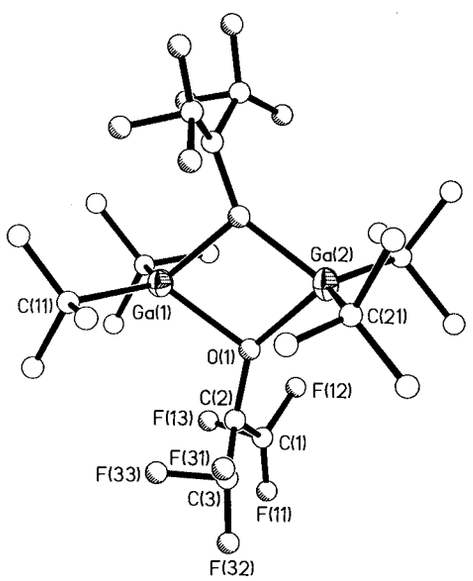


**Fig. 1** Molecular structure of $[(^{t}Bu)_2Ga\{\mu\text{-}OCH(CF_3)_2\}]_2$ (**1**). Thermal ellipsoids are shown at the 30% level, and all hydrogens are omitted for clarity. Selected bond lengths (Å) and angles (°): Ga(1)–O(1) = 2.10(2), Ga(2)–O(1) = 2.02(2); O(1)–Ga(1)–O(1′) = 73.9(9), O(1)–Ga(2)–O(1′) = 77.0(9), Ga(1)–O(1)–Ga(2) = 104.5(4).

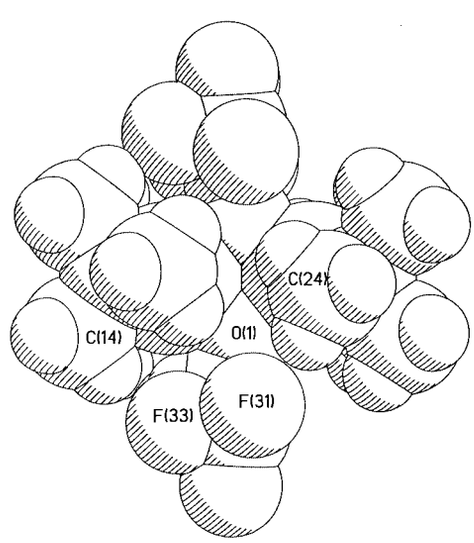


**Fig. 2** Space filling representation of $[(^{t}Bu)_2Ga\{\mu\text{-}OCH(CF_3)_2\}]_2$ (**1**) viewed perpendicular to the $Ga_2O_2$ plane.

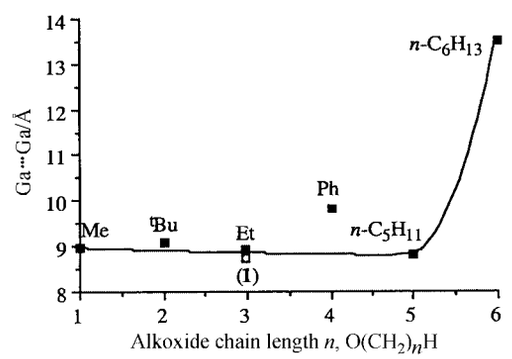


**Fig. 3** A plot of the Ga · · · Ga distance (Å) *versus n*, the length of the alkoxide substituent R, for the dimeric compounds $[(^{t}Bu)_2Ga(\mu\text{-}OR)]_2$.

## Carboxylates

In contrast to the extensive carboxylate chemistry reported for aluminium (and a lesser extent indium) there are only a few examples of organometallic carboxylates for gallium. Reaction of $GaMe_3$ with acetic acid yields the monoacetate, $Me_2Ga(O_2CMe)$, while the addition of excess acid to $Me_3Ga(OEt_2)$ gives the diacetate, $MeGa(O_2CMe)_2$.[13] The structure of the latter was determined by X-ray crystallography to be a mixture of two gallium species having different coordinate geometries; trigonal bipyramidal $GaO_4C$ and distorted tetrahedral $GaO_3C$. The gallium–phenyl analogs have also been reported.

As noted in the Introduction we have previously reported the structural characterization of the di-*tert*-butylgallium benzoates; $[(^{t}Bu)_2Ga(\mu\text{-}O_2CR)]_2$ (R = Ph, $C_6H_4$CN-3 and $C_6H_4$-Br-3),[14] we now report the synthesis and structural characterization of the aliphatic carboxylates, $[(^{t}Bu)_2Ga(\mu\text{-}O_2CR)]_2$ where R = Et (**2**) and $CF_3$ (**3**), prepared in analogous manner to other gallium carboxylates previously prepared in our group.[14] The $^{1}$H and $^{13}$C NMR spectroscopy and mass spectrometry of compounds **2** and **3** are consistent with dimeric structures, which have been confirmed by X-ray crystallography.

The molecular structures of compounds **2** and **3** are shown in Fig. 4 and 5; selected bond lengths and angles are given in Table 1. The structures of both compounds consists of centrosymmetric dimers of two "$Ga(^{t}Bu)_2$" units bridged by two carboxylate groups. This is consistent with other alkyl Group 13 carboxylates as shown from IR and Raman spectroscopy, mass spectrometry, and molecular weight measurements.[15] The Ga–O bond lengths to the carboxylate ligands in these dimeric systems [Ga–O = 1.958(5)–1.984(5) Å] are comparable to the benzoate derivatives [1.957(3)–1.960(3) Å],[14] and to other gallium carboxylates.[16,17] The carboxylate's O–C bond lengths

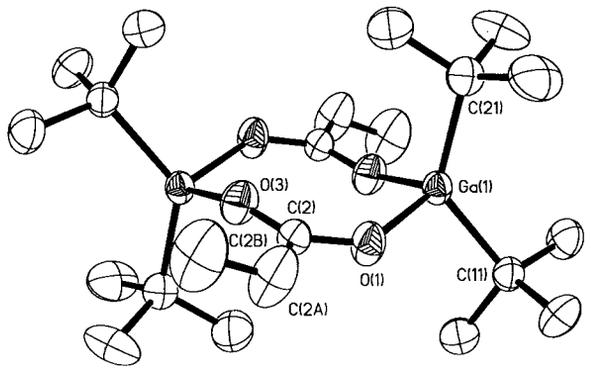


**Fig. 4** Molecular structure of $[(^tBu)_2Ga(\mu\text{-}O_2CEt)]_2$ (**2**). Thermal ellipsoids are shown at the 30% level, and all hydrogens are omitted for clarity.

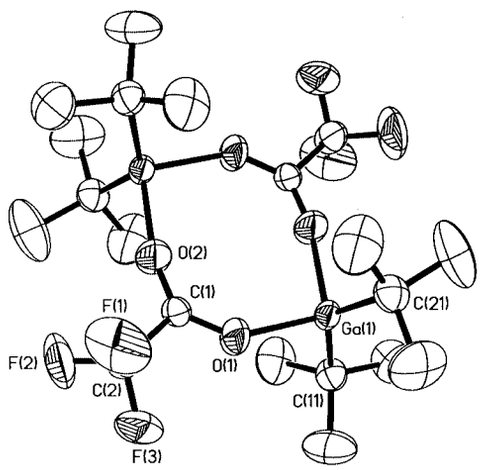


**Fig. 5** Molecular structure of $[(^tBu)_2Ga(\mu\text{-}O_2CCF_3)]_2$ (**3**). Thermal ellipsoids are shown at the 30% level, and all hydrogens are omitted for clarity.

**Table 1** Selected bond lengths (Å) and angles (°) in $[(^tBu)_2Ga(\mu\text{-}O_2CR)]_2$

| $[(^tBu)_2Ga(\mu\text{-}O_2CEt)]_2$ (**2**) | | $[(^tBu)_2Ga(\mu\text{-}O_2CCF_3)]_2$ (**3**) | |
|---|---|---|---|
| Ga(1)–O(1) | 1.960(5) | Ga(1)–O(1) | 1.984(5) |
| Ga(1)–O(3′) | 1.958(5) | Ga(1)–O(2′) | 1.976(5) |
| Ga(1)–C(11) | 1.982(7) | Ga(1)–C(11) | 1.956(7) |
| Ga(1)–C(21) | 1.973(8) | Ga(1)–C(21) | 1.967(8) |
| O(1)–C(2) | 1.242(7) | O(1)–C(1) | 1.214(7) |
| O(3)–C(2) | 1.210(7) | O(2)–C(1) | 1.185(7) |
| | | | |
| O(1)–Ga(1)–O(3′) | 105.0(2) | O(1)–Ga(1)–O(2′) | 102.2(2) |
| O(1)–Ga(1)–C(11) | 103.0(2) | O(1)–Ga(1)–C(11) | 103.3(3) |
| O(1)–Ga(1)–C(21) | 107.4(3) | O(1)–Ga(1)–C(21) | 105.1(3) |
| O(3′)–Ga(1)–C(11) | 101.8(2) | O(2′)–Ga(1)–C(11) | 103.0(3) |
| O(3′)–Ga(1)–C(21) | 107.3(3) | O(2′)–Ga(1)–C(21) | 104.5(3) |
| C(11)–Ga(1)–C(21) | 130.0(3) | C(11)–Ga(1)–C(21) | 134.7(4) |
| Ga(1)–O(1)–C(2) | 137.0(4) | Ga(1)–O(1)–C(1) | 143.7(5) |
| Ga(1′)–O(3)–C(2) | 152.1(5) | Ga(1′)–O(2)–C(1) | 163.4(6) |
| O(1)–C(2)–O(3) | 125.8(6) | O(1)–C(1)–O(2) | 129.8(6) |

in both compounds are similar [Δ(O–C) ≈ 0.03 Å], indicative of a symmetrically bound acid group that is unaffected by the carboxylate organic substituents. The bond lengths and angles within the carboxylate unit are typical of such moieties.

### Amides and phosphoramides

The isostructural relationship between carboxylic acids and protic amides suggests that similar eight-membered cyclic structures would be formed from their reaction with $Ga(^tBu)_3$. The reaction of gallium alkyls with compounds containing N–H bonds are well documented with respect to amines,[18] although the reaction of other N–H acids has also been investigated, including, acetamides, pyrazoles, aza-crown ethers, and tetra-aza macrocycles.

The reaction of one molar equivalent of both benzamide $[PhC(O)NH_2]$ and *N*-phenylacetamide [MeC(O)NHPh] with tri-*tert*-butylgallium does indeed yield bridged dimeric species; $[(^tBu)_2Ga\{\mu\text{-}OC(Ph)N(H)\}]_2$ (**4**) and $[(^tBu)_2Ga\{\mu\text{-}OC(Me)NPh\}]_2$ (**5**), respectively. The $^1H$ and $^{13}C$ NMR spectroscopy and mass spectroscopy of compound **5** are consistent with a single dimeric structure which has been confirmed by X-ray crystallography, see below. In contrast, the $^1H$ and $^{13}C$ NMR spectra of compound **4** reveals the presence of two species in solution. The first appears to be isostructural with that of compound **5**, and involves a centrosymmetric structure with a head-to-tail arrangement of the benzamide ligands (**4a**). Based upon the NMR spectra the second appears to be the head-to-head isomer (**4b**).

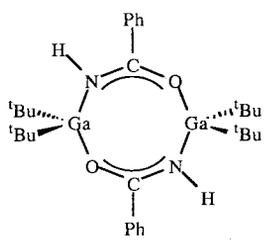


(**4a**)

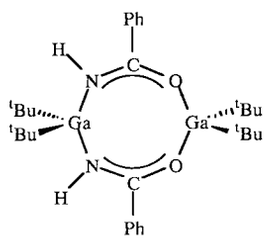


(**4b**)

The molecular structure of compound **4** suggests that both isomers are present in the solid state, see below. This is unlike $[(^tBu)_2Ga(\mu\text{-}OP(S)Ph_2)]_2$ for which the two isomers are separated by repeated recrystallization. The relative ratios of the two isomers as formed for compound **4** are 2:1 (**4a**:**4b**), indicating that the heteroatomic bonding is favored over homoatomic. Similar head-to-tail and head-to-head isomers have been observed previously for similar ligands systems.[20] Mass spectroscopy also indicated the presence of a trimer.

The molecular structures of compounds **4** and **5** are shown in Fig. 6 and 7, respectively. Selected bond lengths and angles for compound **5** are given in Table 2. The bond lengths and angles of the amide ligands are within the ranges observed for similar ligands bonded to other metals.[9] The structures of both compounds involves centrosymmetric dimers with a $Ga_2O_2C_2N_2$ cyclic core. Despite an obvious elongation of the thermal ellipsoids for the nitrogen and oxygen atoms in compound **4**, we were unable to resolve any disorder consistent with the presence of head-to-tail and head-to-head isomers. Two crystallographically independent centrosymmetric molecules are observed in the crystal lattice of $[(^tBu)_2Ga\{\mu\text{-}OC(Ph)N(H)\}]_2$ (**4**). As may be seen from Fig. 8, the difference between these two molecules is due to a variation in the twist of the phenyl rings with respect to the benzamide ligand's O–C–N core, *i.e.*, N(1)–C(11)–C(12)–C(13) = 9.5° and N(4)–C(41)–C(42)–C(43) = 25.5°. Such a difference is presumably as a consequence of inter-molecular packing.

As expected, the reaction of one molar equivalent of $Ga(^tBu)_3$ and *N*,*N*-dimethylbenzamide, $PhC(O)NMe_2$, yields the simple Lewis acid–base complex, $(^tBu)_3Ga[OC(Ph)NMe_2]$ (**6**). The structure of compound **6** is confirmed by $^1H$ and $^{13}C$ NMR and IR spectroscopy as well as X-ray diffraction. The molecular structure of $(^tBu)_3Ga[OC(Ph)NMe_2]$ (**6**) is shown in Fig. 9; selected bond lengths and angles are given in Table 3. Two independent molecules are present in the asymmetric unit; differences between them being due to slight changes in the rotational configuration of the *tert*-butyl ligands (see Fig. 10). The structure consists of a Lewis acid–base adduct with coordination through the amide oxygen atom. The Ga–O distances are significantly longer than in compounds **4** and **5**, while the planar geometry of the benzamide ligand is consistent

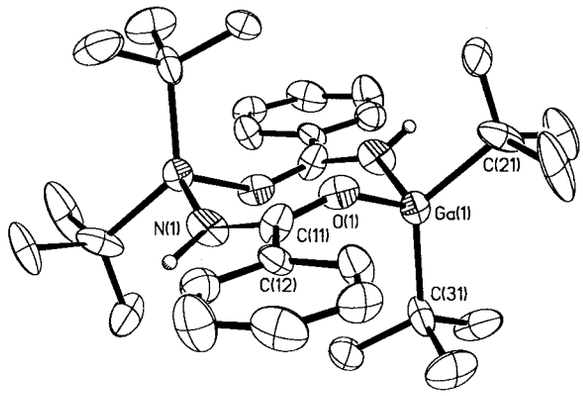


**Fig. 6** Molecular structure of one of the crystallographically independent molecules of $[(^tBu)_2Ga\{\mu\text{-}OC(Ph)N(H)\}]_2$ (**4**). Thermal ellipsoids are shown at the 30% level, and all hydrogens are omitted for clarity. Selected bond lengths (Å) and angles (°): Ga(1)–O(1) = 1.93(2), Ga(2)–O(4) = 1.93(2), Ga(1)–N(1′) = 1.98(2), Ga(2)–N(4′) = 1.95(2); O(1)–Ga(1)–N(1′) = 108.9(9), O(4)–Ga(2)–N(4′) = 99.1(8).

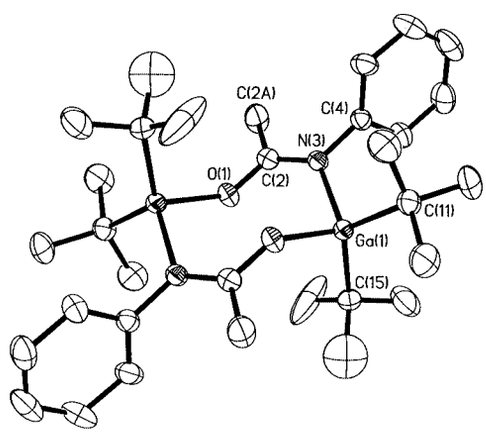


**Fig. 7** Molecular structure of $[(^tBu)_2Ga\{\mu\text{-}OC(Me)NPh\}]_2$ (**5**). Thermal ellipsoids are shown at the 30% level, and all hydrogens are omitted for clarity.

**Table 2** Selected bond lengths (Å) and angles (°) in $[(^tBu)_2Ga\{\mu\text{-}OC(Me)NPh\}]_2$ (**5**)

| | | | |
|---|---|---|---|
| Ga(1)–O(1) | 1.950(3) | Ga(1)–N(3) | 2.023(4) |
| Ga(1)–C(11) | 2.021(5) | Ga(1)–C(15) | 2.016(5) |
| O(1)–C(2) | 1.282(6) | N(3)–C(2) | 1.309(6) |
| N(3)–C(4) | 1.447(6) | | |
| O(1′)–Ga(1)–N(3) | 101.0(2) | O(1)–Ga(1)–C(11) | 99.8(2) |
| O(1)–Ga(1)–C(15) | 109.3(2) | N(3)–Ga(1)–C(11) | 110.0(2) |
| N(3)–Ga(1)–C(15) | 108.4(2) | C(11)–Ga(1)–C(15) | 125.3(2) |
| Ga(1)–O(1)–C(2) | 140.4(3) | Ga(1)–N(3)–C(2) | 122.4(3) |
| Ga(1)–N(3)–C(4) | 117.5(3) | C(2)–N(3)–C(4) | 119.5(4) |
| O(1)–C(2)–N(3) | 120.8(4) | | |

with retention of delocalization of the nitrogen lone pair with the C=O orbitals. The Ga–O–C angles [150.7(5) and 151.4(5)°] are comparable to those observed for organic carbonyl complexes of aluminium.[21] The conformation of the *N*,*N*-dimethylbenzamide with respect to the gallium are the same between both molecules: Ga–O–C–N = 136.7°.

Phosphoramides, $Ph_2P(O)N(H)R$,[22] are clearly iso-electronic to amides and as such would be expected to yield $[(^tBu)_2Ga\{\mu\text{-}OP(Ph)_2NR\}]_2$ upon reaction with $Ga(^tBu)_3$. However, the reaction of $Ph_2P(O)N(H)^nPr$ with $Ga(^tBu)_3$ yields the adduct, $(^tBu)_3Ga[OP(Ph)_2NH(^nPr)]$ (**7**). Both compound **7** and $Ph_2P(O)N(H)^nPr$ were characterized by $^1H$, $^{13}C$, and $^{13}P$ NMR and IR spectroscopy, and mass spectrometry. The N–H resonance is clearly visible in the $^1H$ NMR spectrum and sharpness of the $\nu_{N-H}$ at 3379 $cm^{-1}$ ($W_{\frac{1}{2}} = 11$ $cm^{-1}$) in the IR spectrum indicates very little hydrogen bonding. Instead of converting **7** to $[(^tBu)_2Ga\{\mu\text{-}OP(Ph)_2N^nPr\}]_2$, heating a sample of compound **7** at 100 °C for a day produced only a small amount of decomposition to two unidentified phosphorous containing products. Based upon our previous studies on the parameters that control protonation of Group 13 alkyls,[23] the lack of reactivity of compound **7** may be ascribed to either insufficient activation of the N–H upon coordination, or to insufficient "free" phosphoramide being present in solution. The $^1H$ NMR shift for the N–H ($\delta$ 2.1) is certainly at a higher field than that observed for uncoordinated phosphoramide, suggesting a less acidic proton.

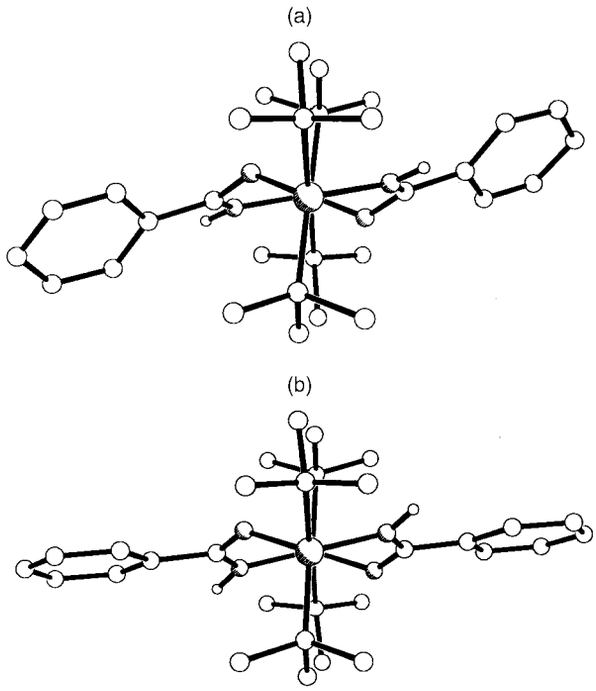


**Fig. 8** The two crystallographic independent molecules observed of $[(^tBu)_2Ga\{\mu\text{-}OC(Ph)N(H)\}]_2$ (**4**) viewed along the Ga · · · Ga vector and showing the variation in the twist of the phenyl rings with respect to the benzamide ligand's O–C–N core.

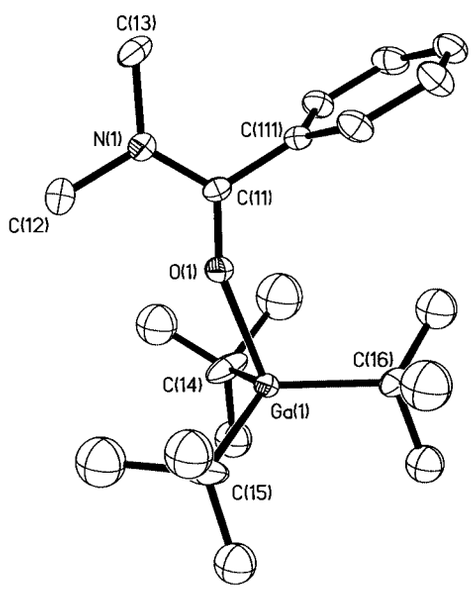


**Fig. 9** Molecular structure of one of the crystallographically independent molecules of $(^tBu)_3Ga[OC(Ph)NMe_2]$ (**6**). Thermal ellipsoids are shown at the 20% level, and all hydrogens are omitted for clarity.

### Benzohydroxamic acid

The reaction of one molar equivalent of benzohydroxamic acid, HON(H)C(O)Ph, with $Ga(^tBu)_3$ gives the compound

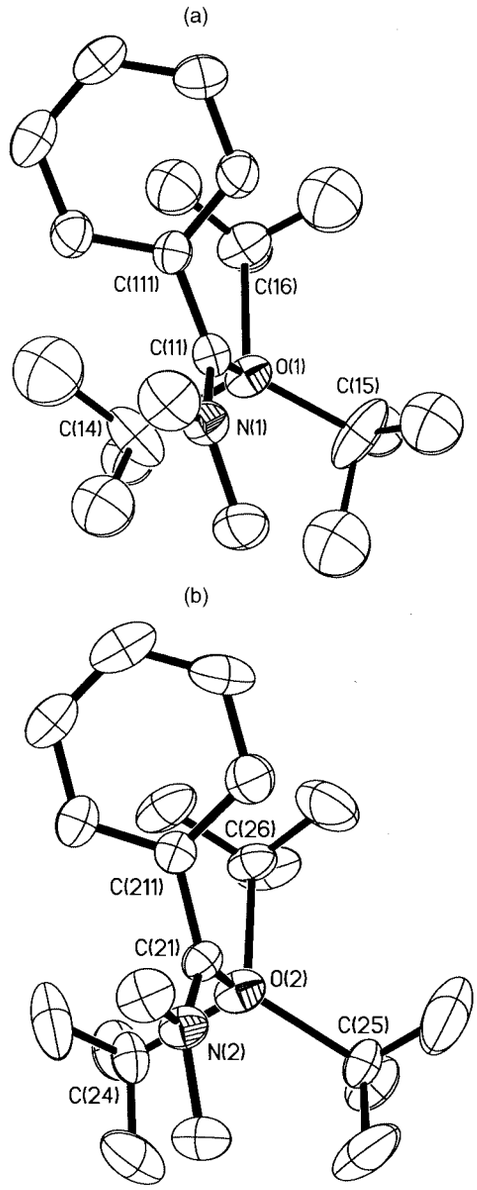


**Fig. 10** Molecular structures of the two crystallographically independent molecules of ($^t$Bu)$_3$Ga[OC(Ph)NMe$_2$] (**6**), viewed along the O–Ga bond showing the different orientation of the *tert*-butyl CH$_3$ groups.

**Table 3** Selected bond lengths (Å) and angles (°) in ($^t$Bu)$_3$Ga[OC(Ph)-NMe$_2$] (**6**)

| Molecule 1 | | Molecule 2 | |
|---|---|---|---|
| Ga(1)–O(1) | 2.133(5) | Ga(2)–O(2) | 2.114(5) |
| Ga(1)–C(14) | 1.979(9) | Ga(2)–C(25) | 2.024(8) |
| Ga(1)–C(15) | 2.002(9) | Ga(2)–C(24) | 2.041(8) |
| Ga(1)–C(16) | 2.043(10) | Ga(2)–C(26) | 2.045(8) |
| O(1)–C(11) | 1.237(7) | O(2)–C(21) | 1.258(8) |
| O(1)–Ga(1)–C(14) | 99.3(3) | O(2)–Ga(2)–C(24) | 98.1(3) |
| O(1)–Ga(1)–C(15) | 97.7(3) | O(2)–Ga(2)–C(25) | 95.8(3) |
| O(1)–Ga(1)–C(16) | 106.2(3) | O(2)–Ga(2)–C(26) | 108.6(3) |
| C(14)–Ga(1)–C(15) | 119.7(7) | C(24)–Ga(2)–C(25) | 116.8(4) |
| C(14)–Ga(1)–C(16) | 114.8(5) | C(24)–Ga(2)–C(26) | 116.2(4) |
| C(15)–Ga(1)–C(16) | 114.8(6) | C(25)–Ga(2)–C(26) | 116.6(4) |
| Ga(1)–O(1)–C(11) | 150.7(5) | Ga(2)–O(2)–C(21) | 151.4(5) |

($^t$Bu)$_2$Ga[ON(H)C(O)Ph] (**8**). This compound was characterized by $^1$H and $^{13}$C NMR and mass spectroscopy, which were consistent with the formation of the monomeric product in solution and the vapor phase. However, the crystal structure as determined by X-ray crystallography shows the presence of

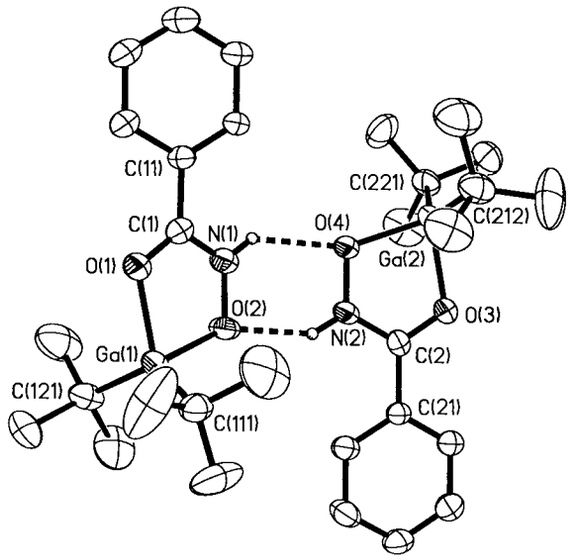


**Fig. 11** Inter-molecular hydrogen bonding between the two crystallographically independent molecules of ($^t$Bu)$_2$Ga[ON(H)C(O)Ph] (**8**). Thermal ellipsoids are shown at the 30% level, and hydrogens bonded to carbon are omitted for clarity.

**Table 4** Selected bond lengths (Å) and angles (°) in ($^t$Bu)$_2$Ga[ON(H)-C(O)Ph] (**8**)

| Molecule 1 | | Molecule 2 | |
|---|---|---|---|
| Ga(1)–O(1) | 1.982(8) | Ga(2)–O(3) | 1.992(7) |
| Ga(1)–O(2) | 1.952(7) | Ga(2)–O(4) | 1.948(7) |
| Ga(1)–C(111) | 1.97(1) | Ga(2)–C(211) | 1.96(1) |
| Ga(1)–C(121) | 1.94(1) | Ga(2)–C(221) | 1.97(1) |
| O(1)–C(1) | 1.28(1) | O(3)–C(2) | 1.25(1) |
| O(2)–N(1) | 1.39(1) | O(4)–N(2) | 1.38(1) |
| N(1)–C(1) | 1.31(1) | N(2)–C(2) | 1.32(1) |
| O(1)–Ga(1)–O(2) | 82.9(3) | O(3)–Ga(2)–O(4) | 81.9(3) |
| O(1)–Ga(1)–C(111) | 108.6(5) | O(3)–Ga(2)–C(211) | 107.5(5) |
| O(1)–Ga(1)–C(121) | 108.4(5) | O(3)–Ga(2)–C(221) | 109.6(5) |
| O(2)–Ga(1)–C(111) | 109.4(5) | O(4)–Ga(2)–C(211) | 110.2(6) |
| O(2)–Ga(1)–C(121) | 107.8(5) | O(4)–Ga(2)–C(221) | 106.4(5) |
| C(111)–Ga(1)–C(121) | 129.7(6) | C(211)–Ga(2)–C(221) | 130.5(6) |
| Ga(1)–O(1)–C(1) | 111.4(7) | Ga(2)–O(3)–C(2) | 111.8(7) |
| Ga(1)–O(2)–N(1) | 107.4(6) | Ga(2)–O(4)–N(2) | 108.6(6) |
| O(2)–N(1)–C(1) | 120(1) | O(4)–N(2)–C(2) | 118.4(9) |
| O(1)–C(1)–N(1) | 118(1) | O(3)–C(2)–N(2) | 119(1) |

hydrogen bonded dimers in the solid state. The retention of the N–H in compound **8** rather than O–H (*i.e.*, ($^t$Bu)$_2$Ga[N(OH)-C(O)Ph]) is indicated by the IR spectrum, see Experimental section.

The molecular structure of ($^t$Bu)$_2$Ga[ON(H)C(O)Ph] (**8**) is shown in Fig. 11; selected bond lengths and angles are given in Table 4. Two independent molecules are observed within the asymmetric unit, in which each gallium is four-coordinate distorted tetrahedral. The largest inter-ligand angle is associated with the *tert*-butyl groups, and the smallest involves the chelate hydroxamate ligand (see Table 4). The difference between the two crystallographically independent molecules is as a result of the relative orientation of the benzohydroxamate phenyl group: C(12)–C(11)–C(1)–O(1) = 20.8° and C(22)–C(21)–C(2)–O(3) = 1.3°. Despite the changes in the orientation of the phenyl groups, the O–C–N–O core of the benzohydroxamates remains constant, *i.e.*, O(1)–C(1)–N(1)–O(2) = 1.6° and O(3)–C(2)–N(2)–O(4) = 1.0°. The solid state crystal packing is dominated by the inter-molecular hydrogen bonding between the two crystallographically independent molecules (Fig. 11). The N···O distances (2.73 and 2.78 Å) are comparable to other N–H···O interactions, however, the O(1)···H(1) distances (1.98 and 2.08 Å) are slightly longer than observed for ketone

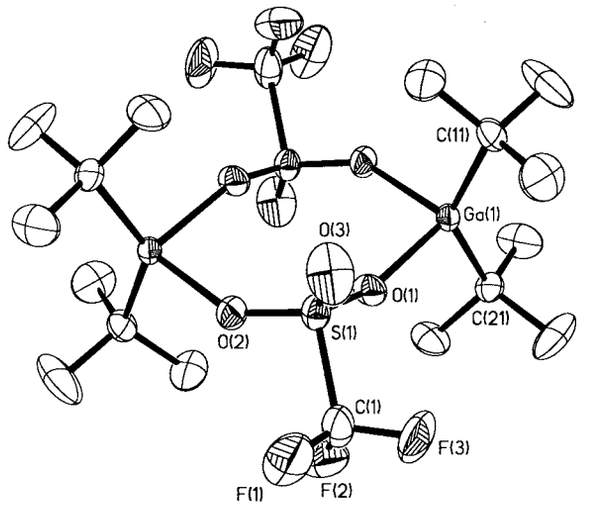


**Fig. 12** Molecular structure of $[(^tBu)_2Ga\{\mu\text{-}O_2S(CF_3)O\}]_2$ (**9**). Thermal ellipsoids are shown at the 30% level, and all hydrogens are omitted for clarity.

**Table 5** Selected bond lengths (Å) and angles (°) in $[(^tBu)_2Ga\{\mu\text{-}O_2S(CF_3)O\}]_2$ (**9**)

| | | | |
|---|---|---|---|
| Ga(1)–O(1) | 2.040(4) | Ga(1)–O(2′) | 2.044(4) |
| Ga(1)–C(11) | 1.970(6) | Ga(1)–C(21) | 1.969(6) |
| S(1)–O(1) | 1.426(4) | S(1)–O(2) | 1.439(4) |
| S(1)–O(3) | 1.403(6) | S(1)–C(1) | 1.84(1) |
| O(1)–Ga(1)–O(2′) | 92.9(2) | O(1)–Ga(1)–C(11) | 108.7(3) |
| O(1)–Ga(1)–C(21) | 101.8(2) | O(2′)–Ga(1)–C(11) | 103.3(3) |
| O(2′)–Ga(1)–C(21) | 105.5(2) | C(11)–Ga(1)–C(21) | 136.4(3) |
| O(1)–S(1)–O(2) | 111.9(3) | O(1)–S(1)–O(3) | 116.2(4) |
| O(1)–S(1)–C(1) | 102.9(4) | O(2)–S(1)–O(3) | 116.1(4) |
| O(2)–S(1)–C(1) | 102.2(4) | O(3)–S(1)–C(1) | 105.3(6) |
| Ga(1)–O(1)–S(1) | 152.6(3) | Ga(1′)–O(2)–S(1) | 144.7(3) |

complexes or trialkylammonium salts, $R_3NH^+ \cdots O{=}CR_2$ (1.72–1.94 Å).[24]

### Triflate

It has been previously shown that gallium triflates are useful Friedel–Crafts catalysts[25] and for the glycosidation of glycopyranosyl fluorides,[26] however, the only structurally characterized gallium triflate has been a monodentate complex.[27] The reaction of $Ga(^tBu)_3$ with one molar equivalent of triflic acid ($CF_3SO_3H$) yields the di-*tert*-butylgallium triflate, $[(^tBu)_2Ga\{\mu\text{-}O_2S(CF_3)O\}]_2$ (**9**). The $^1H$, $^{13}C$, and $^{19}F$ NMR and mass spectra are all consistent with the formulation and the dimeric structure observed in the solid state. No reaction was observed by the addition of excess $CF_3SO_3H$ to compound **9**.

The molecular structure of $[(^tBu)_2Ga\{\mu\text{-}O_2S(CF_3)O\}]_2$ (**9**) is shown in Fig. 12; selected bond lengths and angles are given in Table 5. The triflate ligand bridges two gallium centers in a similar manner to that observed for carboxylates, phosphinates, and amides. The Ga–O distances [2.040(4) and 2.044(4) Å] are slightly longer than those observed for phosphonate and phosphinates [1.969(7)–1.883(8) Å] or carboxylates [1.958(5)–1.984(5) Å].[28,29,30] The S–O distances are surprisingly close given the chemical differences between the intra-ring [1.426(4) and 1.439(4) Å] and exocyclic [1.403(6) Å] oxygens. The closest inter-molecular contact is C–F $\cdots$ F–C at 2.74 Å, which is essentially equivalent to the sum of the van der Waal's radii (2.7 Å).[10]

### Chloride

The Lewis acid properties of gallium and the Lewis basic nature of the chloride ligands results in the formation of stable chloride bridged species. The majority of both mono and di-chloride compounds have been proposed to be dimeric, however, only a few examples have had their structures confirmed by X-ray crystallography.[31] The synthesis of organogallium halides is generally accomplished through three methods which include: (a) reaction of $GaCl_3$ with less than three equivalents of a lithium or Grignard reagent, (b) redistribution reactions between $GaCl_3$ and $GaR_3$, and (c) reaction of $GaR_3$ with HCl. Use of the first of these methods is often complicated by the complexation of LiCl.[32–34] During our investigations into the use of di-*tert*-butylgallium dithiocarbamates, $(^tBu)_2Ga(S_2CNR_2)$, as precursors for the MOCVD growth of GaS,[35] we observed that if the reaction of $[(^tBu)_2Ga(\mu\text{-}Cl)]_2$ with $Li(S_2CN^iPr_2)$ was carried out in the presence of isopropanol (used to clean glassware!) the heterometallic chloride, of $(^tBu)_2Ga(\mu\text{-}Cl)_2\text{-}Li(HO^iPr)_2$ (**10**) was formed in low yield (see Experimental section) which was characterized by X-ray crystallography. The interesting structural character of compound **10** prompted a study of a rational synthesis.

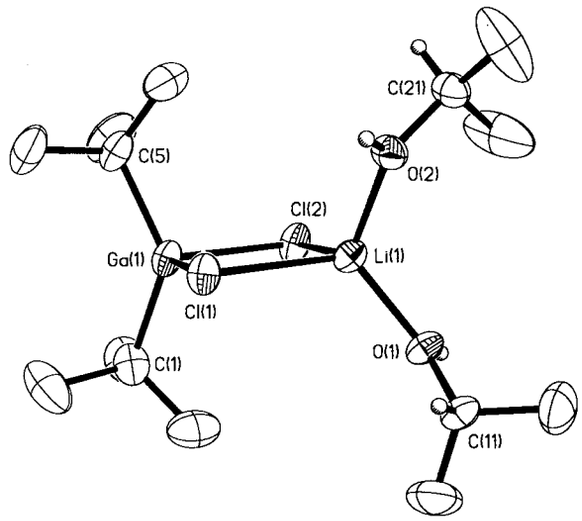


**Fig. 13** Molecular structure of $(^tBu)_2Ga(\mu\text{-}Cl)_2Li(HO^iPr)_2$ (**10**). Thermal ellipsoids are shown at the 20% level, and all hydrogens bonded to carbon are omitted for clarity.

The products formed from the reaction of $GaCl_3$ with two molar equivalents of $^t$BuLi in the presence of $^i$PrOH are dependent on the concentration of the latter (eqn. (1)).

$$GaCl_3 + 2\,{}^t\text{BuLi} \xrightarrow{x\ {}^i\text{PrOH}} [(^tBu)_2GaCl_2][Li(HO^iPr)_n] \quad (1)$$
$$x = 2,\ n = 2\ (\mathbf{10});\ x = \text{excess},\ n = 4\ (\mathbf{11})$$

Thus, if a stoichiometric quantity of $^i$PrOH is employed in the presence of another coordinating solvent, $Et_2O$, compound **10** is formed in modest yield. However, it should be noted that the other (uncharacterized) products were also formed in this reaction, but, due to the presence of the $Et_2O$ these were separated by their preferential solubility in toluene. If excess $^i$PrOH is used, the ionic complex $[Li(HO^iPr)_4][(^tBu)_2GaCl_2]$ (**11**) is formed (see Experimental section).

The molecular structure of $(^tBu)_2Ga(\mu\text{-}Cl)_2Li(HO^iPr)_2$ (**10**) is shown in Fig. 13; selected bond lengths and angles are given in Table 6. The Ga(1)–Cl(1) bond distances [2.333(2) and 2.340(2) Å] are close to the range observed for other $Ga(\mu\text{-}Cl)_2Li$ compounds [2.270(8)–2.302(4) Å].[31] As is commonly observed with dimeric gallium compounds the geometry around gallium in compound **10** is distorted from ideal tetrahedral, with the angles associated with the $Ga(\mu\text{-}Cl)_2Li$ core being the most acute (Table 6). Despite this distortion the torsion angle between the C(1)–Ga–(C5) and Cl(1)–Ga(1)–Cl(2) planes is close to 90°. However, the same is not true for the lithium center. As can also be seen the from Fig. 14, the O(1)–Li(1)–O(2) plane is pitched 14.4° with respect to the Cl(1)–Li(1)–Cl(2)

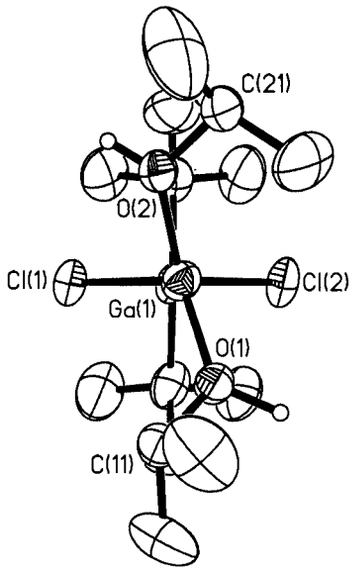


**Fig. 14** Molecular structure of $(^tBu)_2Ga(\mu\text{-}Cl)_2Li(HO^iPr)_2$ (**10**) viewed along the Li(1)···Ga(1) vector showing the distortion about the lithium centers.

**Table 6** Selected bond lengths (Å) and angles (°) in $(^tBu)_2Ga(\mu\text{-}Cl)_2Li(HO^iPr)_2$ (**10**)

| | | | |
|---|---|---|---|
| Ga(1)–Cl(1) | 2.333(2) | Ga(1)–Cl(2) | 2.340(2) |
| Ga(1)–C(1) | 1.986(6) | Ga(1)–C(5) | 1.992(6) |
| Li(1)–Cl(1) | 2.450(8) | Li(1)–Cl(2) | 2.433(8) |
| Li(1)–O(1) | 1.906(8) | Li(1)–O(2) | 1.917(9) |
| Cl(1)–Ga(1)–Cl(2) | 95.69(5) | Cl(1)–Ga(1)–C(1) | 105.9(2) |
| Cl(1)–Ga(1)–C(5) | 107.1(2) | Cl(2)–Ga(1)–C(1) | 106.8(2) |
| Cl(2)–Ga(1)–C(5) | 105.2(2) | C(1)–Ga(1)–C(5) | 130.8(3) |
| Cl(1)–Li(1)–Cl(2) | 90.4(3) | Cl(1)–Li(1)–O(1) | 122.2(4) |
| Cl(1)–Li(1)–O(2) | 101.7(3) | Cl(2)–Li(1)–O(1) | 101.6(3) |
| Cl(2)–Li(1)–O(2) | 118.9(4) | O(1)–Li(1)–O(2) | 119.4(4) |
| Ga(1)–Cl(1)–Li(1) | 86.8(2) | Ga(1)–Cl(2)–Li(1) | 87.1(2) |

plane, resulting in the isopropanol hydrogen atoms being oriented in opposite directions. Similar distortions have been observed in the molecular structures of $[(^tBu)_2In(\mu\text{-}E^tBu)]_2$ (E = S, Se),[36] $[(^tBu)_2Al(\mu\text{-}OPh)]_2$,[37] $[(^tBu)_2Ga(\mu\text{-}OPh)]_2$,[14] $[(^tBu)_2Al\{\mu\text{-}OAl(^tBu)_2\}]_2$,[6] $[(2,4,6\text{-}Me_3C_6H_2)_2In(\mu\text{-}Cl)]_2$,[38] and $[Ph_2In\{\mu\text{-}SSn(C_6H_{11})_3\}]_2$.[39] However, in each of these cases significant intra-molecular steric interaction was observed to be the cause of this twisting away from a tetrahedral geometry. In the case of compound **10** no such steric interactions appear to be present. A consideration of the crystal packing of compound **10** indicates that the orientation of the alcohol ligands allows for an O–H···Cl hydrogen bonding interaction (O···Cl = 3.34 Å) between adjacent molecules, see Fig. 15. The result of this hydrogen bonding is the formation of a series of molecular chains along the crystallographic *a*-axis (Fig. 16). Based upon the hierarchical levels of crystal architecture proposed by Whitesides and co-workers,[40] the structure of $(^tBu)_2Ga(\mu\text{-}Cl)_2Li(HO^iPr)_2$ (**10**) may be described as consisting of a series of head-to-waist (*primary* level) interactions, creating a series of linear tapes (*secondary* level) which are coplanar but contain no inter-tape contacts (*tertiary* level).

The structure of the anion and cation in $[Li(HO^iPr)_4][(^tBu)_2GaCl_2]$ (**11**) are shown in Fig. 17 and 18, respectively. The structure of the $[(^tBu)_2GaCl_2]^-$ anion is similar to that reported for the methyl analog,[41] with the expected increase in the C–Ga–C angle associated with the larger *tert*-butyl groups. The Ga–Cl distances in **11** [2.274(4) and 2.332(4) Å] are similar to those for other terminal anionic chloride species [2.136(4)–2.203(1) Å],[42] but are shorter than in neutral chlorides [1.934(8)–1.99(1) Å].[43–46] The $[Li(HO^iPr)_4]^+$ cation has a near tetrahedral geometry about Li(1), with the Li–O distances being comparable to

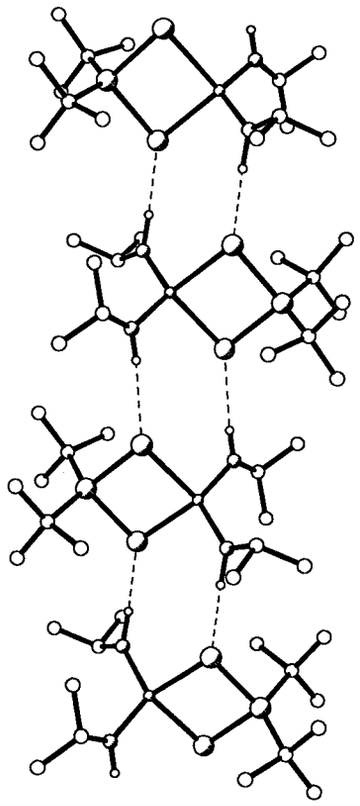

**Fig. 15** Structure of the hydrogen bonded tape of $(^tBu)_2Ga(\mu\text{-}Cl)_2Li(HO^iPr)_2$ (**10**). Hydrogens bonded to carbon are omitted for clarity.

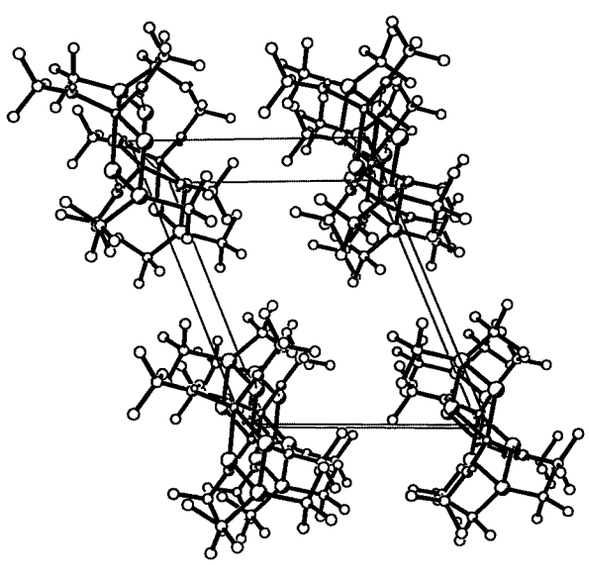

**Fig. 16** View along the crystallographic *a*-axis of $(^tBu)_2Ga(\mu\text{-}Cl)_2Li(HO^iPr)_2$ (**10**) illustrating the series of molecular chains created by the hydrogen bonded tapes.

those observed in compound **10**, see above. As is readily seen from Fig. 18, the isopropanol ligands in the $[Li(HO^iPr)_4]^+$ cation are oriented in pairs in opposite directions. This orientation appears unfavorable due to the steric interactions of the isopropyl groups. However, the orientation is optimum for hydrogen bonding to the anions. Fig. 19 shows one of the cation···anion chains that are formed in the solid state along the crystallographic *b*-axis. It is interesting to note that while Cl(1) is involved in only a single hydrogen bonding interaction (making it formally two coordinate), Cl(2) is involved in three hydrogen bonding interactions. Of these three interactions, one is with the same cation as that coordinated to Cl(1) and the other two are involved with a second cation. The geometry about Cl(2) is therefore close to tetrahedral. The hierarchical

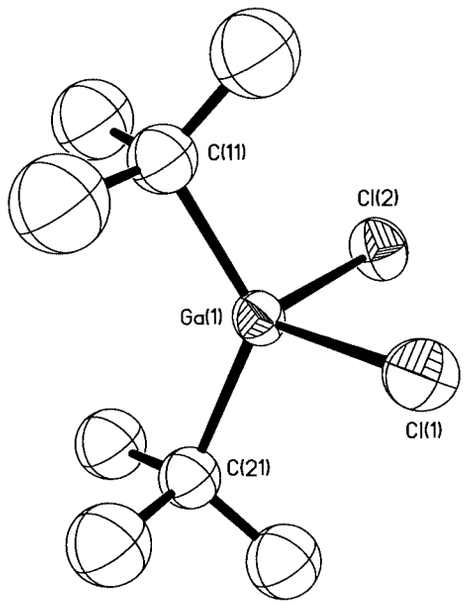


**Fig. 17** Structure of the $[(^tBu)_2GaCl_2]$ anion in **11**. Thermal ellipsoids are shown at the 20% level, and all hydrogens are omitted for clarity. Selected bond lengths (Å) and angles (°): Ga(1)–Cl(1) = 2.274(4), Ga(1)–Cl(2) = 2.332(4), Ga(1)–C(11) = 2.02(2), Ga(1)–C(21) = 2.01(2); Cl(1)–Ga(1)–Cl(2) = 99.5(2), Cl(1)–Ga(1)–C(11) = 107.8(6), Cl(1)–Ga(1)–C(21) = 105.7(6), Cl(2)–Ga(1)–C(11) = 105.8(6), Cl(2)–Ga(1)–C(21) = 105.7(6), C(11)–Ga(1)–C(21) = 128.7(8).

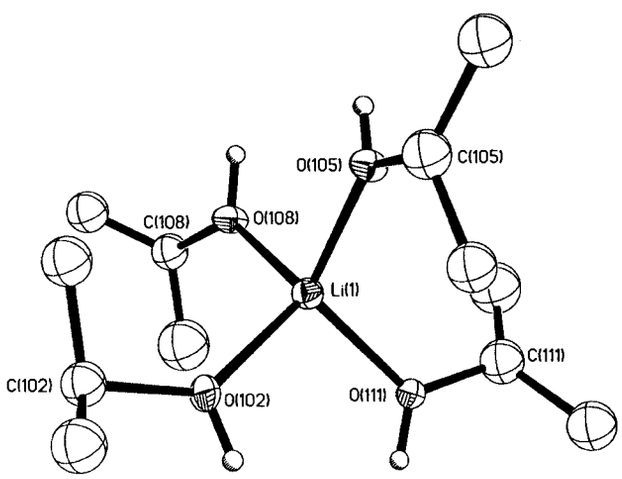


**Fig. 18** Structure of $[Li(HO^iPr)_4]$ cation in **11**. Thermal ellipsoids are shown at the 20% level, and all hydrogens bonded to carbon are omitted for clarity. Li–O = 1.91(3)–1.97(3) Å; O–Li–O = 98(1)–116(2)°.

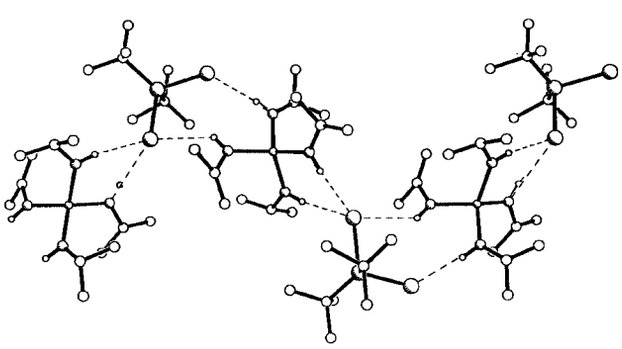

**Fig. 19** Crystal structure of $[Li(HO^iPr)_4][(^tBu)_2GaCl_2]$ (**11**). All hydrogens bonded to carbon are omitted for clarity.

structure of $[Li(HO^iPr)_4][(^tBu)_2GaCl_2]$ (**11**) may therefore be described as consisting of dimers (*primary* level) formed between a cation and anion and containing an eight membered Ga–Cl···H–O–Li–O–H···Cl cycle. These dimers are linked through Cl(2) *via* two further hydrogen bonds to form a helix (*secondary* level). These helices run parallel, but contain no inter-helix contacts (*tertiary* level).

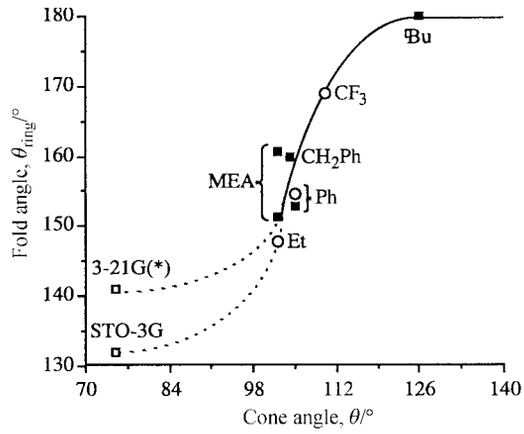


**Fig. 20** Plot of the folding of the $M_2O_4C_2$ cycle ($\theta_{ring}$/°) in the dialkylaluminium (■) and dialkylgallium (○) carboxylates, $[(^tBu)_2M(\mu\text{-}O_2CR)]_2$, *versus* the Tolman's cone angle, $\theta$, of the carboxylate substituent (°). The values calculated at the HF/3-21G(*) and HF STO-3G levels for $[H_2Al(\mu\text{-}O_2CH)]_2$ are included for comparison (□).

## Ring folding

We have previously discussed the dependence of the puckering of the chair-like conformation in Group 13 carboxylates, $[R_2M(\mu\text{-}O_2CR')]_2$ (M = Al, Ga), upon the steric bulk of the substituents on both the metal and the carboxylate, *i.e.*, R and R′, respectively.[47] The puckering of the $M_2O_4C_2$ ring may be considered to be as a result of folding of the eight-membered ring along the two inter-ligand O···O vectors. The extent of folding ($\theta_{ring}$) is defined as the angle between the $MO_2$ planes and the $O_4C_2$ plane. For the aluminium metal carboxylates, $[(^tBu)_2Al(\mu\text{-}O_2CR)]_2$, the geometrical result of the planar $Al_2O_4C_2$ core is that the Al···Al intra-molecular distance is maximized, and consequently so are the inter-substituent distances (*i.e.*, $^tBu\cdots R$), resulting in a correlation between $\theta_{ring}$ and the steric bulk of the carboxylate substituent (R) as defined by Tolman's cone angle ($\theta$).[2] In this regard, a similar trend is observed for the gallium carboxylates, see Fig. 20. As may be seen from Fig. 20, the similarity in the relationships for aluminium and gallium carboxylates is consistent with the similarity in their covalent radii. It is interesting to note that the observed fold angle of $[(^tBu)_2Ga(\mu\text{-}O_2CCF_3)]_2$ ($\theta_{ring}$ = 168.6°), is significantly larger than may be expected given that the cone angle for $P(CF_3)_3$ (137°) is intermediate between $PEt_3$ (132°) and $PPh_3$ (145°). Based upon the phosphine values, the cone angle of the $CF_3$ group would be expected to be 102–105°. However, given the similarity in the steric bulk of Me and F, the cone angle of $CF_3$ would indeed be expected to be similar to that of $C(CH_3)_3$, which is observed for the carboxylate compounds of the Group 13 metals.

As described above, the triflate and amides are also examples of eight-membered ring compounds of the Group 13 metals.[48] The fold angle ($\theta_{ring}$) for $[(^tBu)_2Ga\{\mu\text{-}O_2S(CF_3)O\}]_2$ (**9**), $[(^tBu)_2Ga\{\mu\text{-}OC(Ph)N(H)\}]_2$ (**4**) and $[(^tBu)_2Ga\{\mu\text{-}OC(Me)NPh\}]_2$ (**5**) are 161.5°, 134.1° and 126.4°, respectively. While the value for the triflate ligand is comparable to that of the carboxylates, those of the amides, compounds **4** and **5**, are significantly lower. This is as expected given the presence of substituents on the amide nitrogen. Furthermore, the substitution of H in $[(^tBu)_2Ga\{\mu\text{-}OC(Ph)N(H)\}]_2$ (**4**) with Ph in $[(^tBu)_2Ga\{\mu\text{-}OC(Me)NPh\}]_2$ (**5**) results in a greater folding of the ring as a consequence of the repulsion between the gallium *tert*-butyl groups and the phenyl ring. This is clearly seen in Fig. 21, in which the Ga–C bonds are almost perfectly staggered with respect to the N(3)–C(2) bond.

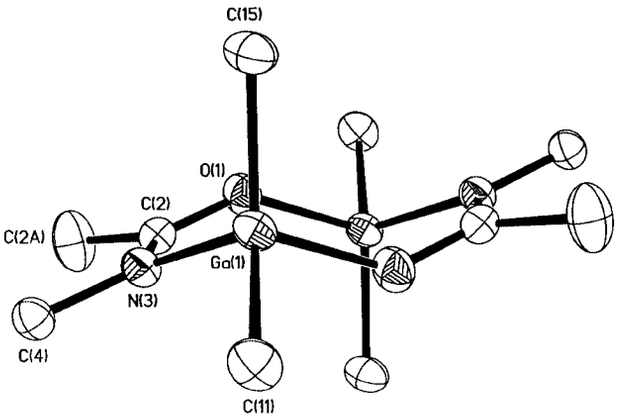


**Fig. 21** Structure of $[(^tBu)_2Ga\{\mu\text{-}OC(Me)NPh\}]_2$ (**5**) demonstrating the staggered conformation of N(3)–C(2) with respect to the two Ga–C bonds.

## Experimental

Mass spectra were obtained on a Finnigan MAT 95 mass spectrometer operating with an electron beam energy of 70 eV for EI mass spectra. IR spectra (4000–400 $cm^{-1}$) were obtained using an Nicolet 760 FT-IR infrared spectrometer. IR samples were prepared as Nujol mulls between NaCl plates unless otherwise stated. NMR spectra were obtained on Bruker AM-250 and Avance 200 spectrometers using (unless otherwise stated) $d_6$-benzene solutions. Chemical shifts are reported relative to internal solvent resonances ($^1H$ and $^{13}C$), and external $CFCl_3$ ($^{19}F$) and $H_3PO_4$ ($^{31}P$). The synthesis of $Ga(^tBu)_3$ was performed according to the literature methods.[49] $HOCH(CF_3)_2$, $HO_2CEt$, $HO_2CCF_3$, and MeC(O)NHOPh were obtained from Aldrich and were used without further purification. PhP(O)N(H)Et was prepared by the literature method.[50]

### Syntheses

**$[(^tBu)_2Ga\{\mu\text{-}OCH(CF_3)_2\}]_2$ (1).** To a solution of $Ga(^tBu)_3$ (4.5 g, 18.7 mmol) in hexane (40 $cm^3$) was added $HOCH(CF_3)_2$ (2.0 $cm^3$, 19 mmol), *via* syringe at −78 °C. After the solution was warmed to room temperature and stirred for 1.5 h, the volume of the solution was reduced and set aside in the freezer (−20 °C) overnight. Colorless, X-ray quality crystals formed. Yield: 3.50 g, 52%. Mp 64 °C. MS (EI, %): *m/z* 567 [$2M^+ - CH(CF_3)_2 + O$, 77], 437 [$2M^+ - 2\ ^tBu - CH(CF_3)_2$, 20], 343 [$2M^+ - {}^tBu - 2\ CH(CF_3)_2$, 75], 183 [$M^+ - OCH(CF_3)_2$, 100]. IR ($cm^{-1}$): 1296 (s), 1237 (s), 1202 (s), 1102 (s), 1010 (w), 943 (w), 933 (w), 894 (m), 867 (m), 812 (m), 748 (m), 691 (m), 634 (w). $^1H$ NMR: $\delta$ 4.75 [2H, sept, $J$(H–F) = 6.0 Hz, $OCH(CF_3)_2$], 0.93 [36H, s, $C(CH_3)_3$]. $^{13}C$ NMR: $\delta$ 123.5 [q, $J$(C–F) = 284 Hz, $OCH(CF_3)_2$], 74.2 [sept, $J$(C–F) = 31.8 Hz, $OCH(CF_3)_2$], 31.8 [$C(CH_3)_3$], 29.0 [$C(CH_3)_3$]. $^{19}F$ NMR: $\delta$ −76.62 [d, $J$(H–F) = 6.0 Hz, $OCH(CF_3)_2$].

**$[(^tBu)_2Ga(\mu\text{-}O_2CEt)]_2$ (2).** $EtCO_2H$ (1.4 $cm^3$, 19 mmol) was added, *via* syringe, to a solution of $Ga(^tBu)_3$ (4.50 g, 18.7 mmol) in hexane (40 $cm^3$) at −78 °C. After the solution was warmed to room temperature and stirred for 2 h, all volatiles were removed under vacuum leaving a white solid. Yield: 4.00 g, 83%. Mp 104–105 °C. MS (EI, %): *m/z* 457 ($2M^+ - {}^tBu$, 3), 417 ($2M^+ - CH_2{=}CMe_2 - CCH_2CH_3$, 10), 401 ($2M^+ - CH_2{=}CMe_2 - OCCH_2CH_3$, 9), 343 ($2M^+ - 2\ CH_2{=}CMe_2 - O_2CCH_2CH_3$, 5), 256 ($M^+$, 20), 199 ($M^+ - {}^tBu$, 30), 143 ($M^+ - {}^tBu - CH_2{=}CMe_2$, 100), 57.1 ($^tBu$, 75). IR ($cm^{-1}$): 2709 (w), 1596 (s), 1437 (s), 1364 (m), 1306 (m), 1243 (w), 1180 (w), 1083 (m), 1011 (m), 943 (w), 895 (w), 818 (m), 721 (w). $^1H$ NMR: $\delta$ 2.17 [4H, q, $J$(H–H) = 7.5 Hz, $O_2CCH_2$], 1.20 [ 36H, s, $C(CH_3)_3$], 0.95 [6H, t, $J$(H–H) = 7.5 Hz, $O_2CCH_2CH_3$]. $^{13}C$ NMR: $\delta$ 185.6 ($O_2C$), 31.3 ($O_2CCH_2$), 30.1 [$C(CH_3)_3$], 24.3 [$C(CH_3)_3$], 10.0 ($O_2CCH_2CH_3$).

**$[(^tBu)_2Ga(\mu\text{-}O_2CCF_3)]_2$ (3).** A solution of $CF_3CO_2H$ (0.543 g, 5.32 mmol) in hexane (20 $cm^3$) was added, *via* cannula, to $Ga(^tBu)_3$ (1.28 g, 5.31 mmol) in hexane (30 $cm^3$). After the clear colorless solution was stirred overnight, the volume of solvent was reduced under vacuum to about 5 mL and set aside in the freezer (−20 °C). Colorless, X-ray quality crystals formed. Yield: 3.50 g, 46%. Mp 126–127 °C. MS (EI, %): *m/z* 537 ($2M^+ - {}^tBu$, 2), 497 ($2M^+ - OCCF_3$, 10), 441 ($2M^+ - OCCF_3 - CH_2{=}CMe_2$, 3), 383 ($2M^+ - OCCF_3 - 2\ ^tBu$, 3), 327 ($2M^+ - OCCF_3 - 2\ ^tBu - CH_2{=}CMe_2$, 3), 296 ($M^+$, 4), 239 ($M^+ - {}^tBu$, 2), 183 ($M^+ - O_2CCF_3$, 25), 57 ($^tBu$, 100). IR ($cm^{-1}$): 3168 (w), 3124 (w), 2723 (w), 1693 (s), 1369 (m), 1209 (s), 1175 (s), 1020 (m), 948 (w), 852 (m), 821 (m), 790 (m), 730 (s), 624 (m). $^1H$ NMR: $\delta$ 1.09 [36H, s, $C(CH_3)_3$]. $^{13}C$ NMR: $\delta$ 164.7 [q, $J$(C–F) = 41.5 Hz, $O_2CCF_3$], 116.0 [q, $J$(C–F) = 287 Hz, $O_2CCF_3$], 29.0 [$(C(CH_3)_3$], 25.9 [$(C(CH_3)_3$]. $^{19}F$ NMR: $\delta$ −75.27 (s, $O_2CCF_3$).

**$[(^tBu)_2Ga\{\mu\text{-}OC(Ph)N(H)\}]_2$ (4).** A solution of $Ga(^tBu)_3$ (1.0 g, 4.17 mmol) in hexane (10 $cm^3$) was added to a solution of benzamide (0.50 g, 4.13 mmol) in hexane (20 $cm^3$). Upon addition a yellow solution was immediately observed, and the solution became warm to the touch. This resulting mixture was then heated to reflux for 30 min. This was allowed to cool, and a white percipitate was observed upon cooling to room temperature. The resulting mixture was allowed to stir overnight (10 h). Removal of all volatiles yielded a white powder, which was recrystallized from $CH_2Cl_2$ to give clear, block crystals. Yield: *ca.* 80%. Mp 174–176 °C. MS (EI, %): *m/z* 551 ($2M^+ - {}^tBu$, 5), 448 ($M^+ + {}^tBuGaNH_2$, 10), 303 ($M^+ + H$, 3), 246 ($M^+ - {}^tBu + H$, 80), 190 ($M^+ - 2\ ^tBu + H$, 95), 103 (PhCN, 70), 69 (Ga, 65), 57 ($^tBu$, 100). IR ($cm^{-1}$): 3375 (s), 1598 (m), 1557 (m), 1501 (m), 1296 (s), 1235 (s), 1173 (s), 1137 (s), 1091 (s), 1066 (s), 968 (s), 938 (s), 815 (s), 702 (m), 666 (s). $^1H$ NMR: $\delta$ **A** 7.72 [2H, d, $J$(H–H) = 5.3 Hz, *o*-C*H*], 7.03 [3H, m, $J$(H–H) = 5.3 Hz, *m*-C*H*, *p*-C*H*], 6.55 (2H, s, N*H*), 1.26 [18H, s, $C(CH_3)_3$]. **B** 7.80 [2H, d, $J$(H–H) = 6.0 Hz, *o*-C*H*], 6.61 (2H, s, N*H*), 1.31 [18H, s, $N_2GaC(CH_3)_3$], 1.30 [18H, s, $O_2GaC(CH_3)_3$]. $^{13}C$ NMR: $\delta$ **A** 206.8 (*C*ON), 132.2 (*o*-*C*H), 129.4 (*m*-*C*H), 129.3 (*p*-*C*H), 31.4 [$C(CH_3)_3$], 24.3 [$C(CH_3)_3$]. **B** 31.8 [$N_2GaC(CH_3)_3$], 31.1 [$O_2GaC(CH_3)_3$].

**$[(^tBu)_2Ga\{\mu\text{-}OC(Me)NPh\}]_2$ (5).** A solution of MeC(O)NHPh (0.561 g, 4.15 mmol) in toluene (30 $cm^3$) was added, *via* cannula, to a cooled (0 °C) hexane (10 $cm^3$) solution of $Ga(^tBu)_3$ (1.00 g, 4.15 mmol). After the clear colorless solution was refluxed for 2 h, the volume of solvent was reduced under vacuum and set aside in the freezer (−20 °C) resulting in the formation of colorless, X-ray-quality crystals. Yield: 53%. Mp: 143–145 °C. MS (EI, %): *m/z* 578.7 ($2M^+ - {}^tBu$, 42), 260 ($M^+ - {}^tBu$, 20), 204 ($M^+ - {}^tBu - CH_2{=}C(CH_3)_2$, 30), 118 ($CH_3CNPh$, 100). IR ($cm^{-1}$): 1606 (w), 1543 (s), 1233 (m), 1069 (w), 1011 (w), 963 (w), 919 (w), 846 (m), 813 (m), 764 (m), 701 (m), 672 (w). $^1H$ NMR: $\delta$ 7.06 [4H, m, $N(C_6H_5)$], 6.88 [6H, m, $N(C_6H_5)$], 1.68 [6H, s, $OCCH_3$], 1.32 [36H, s, $C(CH_3)_3$]. $^{13}C$ NMR: $\delta$ 179.8 (O*C*), 144.3 [$N(C_6H_5)$], 129.6 [$N(C_6H_5)$], 125.1 [$N(C_6H_5)$], 124.4 [$N(C_6H_5)$], 30.1 [$C(CH_3)_3$], 25.1 [$C(CH_3)_3$], 18.0 [$OC(CH_3)$].

**$(^tBu)_3Ga[OC(Ph)NMe_2]$ (6).** A slurry of $PhC(O)NMe_2$ (0.62 g, 4.16 mmol) in hexane (20 $cm^3$) was cooled to −78 °C with continuous stirring. To this was added dropwise a solution of $Ga(^tBu)_3$ (1.0 g, 4.17 mmol) in hexane (5 $cm^3$). The presence of the ligand was seen to disappear as the mixture was allowed to slowly come to room temperature. The resulting clear solution was allowed to stir 36 h, then the volatiles were removed to leave a clear gel which formed large rectangular crystals under vacuum. These were recrystallized in a small amount of toluene to give clear rectangular crystals. Yield: *ca.* 90%. Mp 72–73 °C. $^1H$ NMR: $\delta$ 6.98 [5H, m, $J$(H–H) = 2.59 Hz, C–*H*], 2.59 (3H, s,

NC$H_3$), 1.89 (3H, s, NC$H_3$), 1.28 [27H, s, C(C$H_3$)$_3$]. $^{13}$C NMR ($CDCl_3$): $\delta$ 218.5 (ONCO), 129.0 (*o*-CH), 128.9 (*m*-CH), 127.0 (*p*-CH), 31.8 [C(CH$_3$)$_3$], 31.1 [C(CH$_3$)$_3$].

**($^t$Bu)$_3$Ga[OP(Ph)$_2$NH($^n$Pr)] (7).** A solution of $Ph_2P(O)NH(^nPr)$ (0.761 g, 2.91 mmol) in toluene (20 cm$^3$) was added, *via* cannula, to Ga($^t$Bu)$_3$ (0.701 g, 2.91 mmol) in hexane (20 cm$^3$) at −78 °C. After the solution was stirred at −78 °C for 45 min, it was warmed to room temperature and was stirred for another 2 h. The volatiles were then removed under vacuum and the resulting white solid was recrystallized from hexane yielding X-ray-quality crystals. Yield 17%. Mp 106–109 °C. MS (EI, %): *m*/*z* 457 ($Ga_2{}^tBu_2Ph_2PO$ + 2 H, 95), 401 ($Ga_2{}^tBuPh_2PO$ + 3 H, 70), 345 ($Ga_2Ph_2PO$ + 4 H, 100), 271 ($^t$BuGaONPr, 70), 259 ($Ph_2PONHPr$, 100). IR (cm$^{-1}$): 3379 (s), 2690 (w), 1591 (w), 1410 (m), 1378 (s), 1359 (w), 1237 (w), 1163 (s), 1130 (s), 1110 (s), 1085 (m), 1030 (w), 1011 (w), 934 (w), 904 (w), 812 (m), 754 (m), 748 (w), 695 (m). $^1$H NMR: $\delta$ 7.8 [4H, m, P(C$_6H_5$)], 7.0 [6H, m, P(C$_6H_5$)], 2.70 [2H, m, NC$H_2$], 2.1 [1H, m, NH], 1.50 [27H, s, C(C$H_3$)$_3$], 1.09 [2H, tq, *J*(H–H) = 7.4 Hz, *J*(H–H) = 7.4 Hz, NCH$_2$C$H_2$], 0.53 [3H, t, *J*(H–H) = 7.4 Hz, NCH$_2$CH$_2$C$H_3$]. $^{13}$C NMR: $\delta$ 133.3 [s, P(C$_6$H$_5$)], 133.1 [d, *J*(C–P) = 10 Hz, P(C$_6$H$_5$)], 129.4 [d, *J*(C–P) = 13 Hz, P(C$_6$H$_5$)], 43.8 (s, NCH$_2$CH$_2$), 33.6 [s, C(CH$_3$)$_3$], 25.5 [d, *J*(C–P) = 8 Hz, NCH$_2$], 25.1 [s, C(CH$_3$)$_3$], 11.6 (s, NCH$_2$CH$_2$CH$_3$). $^{31}$P NMR: $\delta$ 26.6 (s).

**($^t$Bu)$_2$Ga[ON(H)C(O)Ph] (8).** A slurry of HON(H)C(O)Ph (0.52 g, 3.82 mmol) in hexane (15 cm$^3$) was cooled to −78 °C with continuous stirring. To this mixture was added Ga($^t$Bu)$_3$ (1.0 g, 4.17 mmol) in hexane (5 cm$^3$). Evolution of gas was seen upon this addition, and the white powder present in the bottom of the flask disappeared as the mixture was allowed to slowly warm to room temperature. After stirring overnight (12 h) the mixture was filtered. Removal of all volatiles from the filtrate yielded a white powder, which was recrystallized in toluene to give clear hexagonal-shaped crystals. Yield: *ca*. 70%. Mp 149–150 °C. MS (EI, %): *m*/*z*: 319 (M$^+$, 2), 262 (M$^+$ − $^t$Bu, 75), 206 (M$^+$ − 2 $^t$Bu, 100), 103 (PhCN, 30), 57 ($^t$Bu, 35). IR (cm$^{-1}$): 3202 (w), 3134 (w), 1601 (m), 1582 (m), 1533 (m), 1483 (m), 1364 (m), 1310 (s), 1141 (m), 1050 (m), 1030 (m), 903 (m), 817 (s), 779 (s), 726 (s), 692 (m), 663 (s). $^1$H NMR: $\delta$ 7.40 [2H, d, *J*(H–H) = 6.75 Hz, *o*-CH], 6.96 [3H, m, *J*(H–H) = 6.75 Hz, *m*-CH, *p*-CH], 1.35 [18H, s, C(C$H_3$)$_3$]. $^{13}$C NMR: $\delta$ 193.8 (ONCO), 132.4 (*o*-CH), 129.3 (*m*-CH), 126.8 (*p*-CH), 30.2 [C(CH$_3$)$_3$], 25.0 [C(CH$_3$)$_3$].

**[($^t$Bu)$_2$Ga{μ-O$_2$S(CF$_3$)O}]$_2$ (9).** Upon addition of $CF_3SO_3H$ (4.845 g, 32.3 mmol) to a solution of Ga($^t$Bu)$_3$ (7.78 g, 32.3 mmol) in hexane (50 cm$^3$), two layers formed immediately. As the lower (yellow) layer gradually diminished, the solution became warm. After about 15 min a small amount of the lower layer remained and the top layer was faint yellow. The mixture was stirred for another hour during which time there was no further change. The volatiles were removed under vacuum yielding a white solid coated with a yellow oil. The solid was sublimed under vacuum at 75 °C to remove the yellow oil. Colorless, X-ray quality crystals were grown from a hexane solution at −20 °C. Yield 84%. Mp 141–143 °C. MS (EI, %): *m*/*z* 609 (2M$^+$ − $^t$Bu, 10), 495 (2M$^+$ − 3 $^t$Bu, 10), 289 (2M$^+$ − 4 $^t$Bu − O$_3$SCF$_3$, 10), 183 (M$^+$ − O$_3$SCF$_3$, 70), 57 ($^t$Bu, 100). IR (cm$^{-1}$): 1337 (s), 1230 (s), 1208 (s), 1167 (s), 1032 (s), 1011 (s), 944 (w), 815 (m), 808 (m), 634 (s). $^1$H NMR: $\delta$ 1.64 [s, C(C$H_3$)$_3$]. $^{13}$C NMR: $\delta$ 119.4 [q, *J*(C–F) = 317 Hz, O$_3$SCF$_3$], 28.5 [s, C(CH$_3$)$_3$], 27.8 [s, C(CH$_3$)$_3$]. $^{19}$F NMR: $\delta$ −76.69 (s, O$_3$SCF$_3$).

**($^t$Bu)$_2$Ga(μ-Cl)$_2$Li(HO$^i$Pr)$_2$ (10).** *Method 1.* A solution of Li(S$_2$CN$^i$Pr$_2$) (0.70 g, 3.8 mmol) in hexane (20 cm$^3$) was cooled to −78 °C, and to this was added [($^t$Bu)$_2$Ga(μ-Cl)]$_2$ (0.90 g, 4.11 mmol) in hexane (20 cm$^3$) dropwise. The resulting solution was slowly brought to room temperature, allowed to stir overnight (10 h), and then filtered into $^i$PrOH contaminated glassware. The resulting filtrate was removed of its volatiles to yielded a yellow liquid, which, when cooled to −20 °C gave a yellow oil and a solid. This was then recrystallized in toluene to give clear block crystals.

*Method 2.* $GaCl_3$ (1.0 g, 5.7 mmol) in $Et_2O$ (10 cm$^3$) was cooled to −78 °C, to which $^t$BuLi solution (6.7 cm$^3$, 1.7 M in pentane, 11.4 mmol) was added dropwise. The resulting mixture was allowed to come to room temperature with continuous stirring, then $^i$PrOH (1.0 cm$^3$, 0.785 g, 13.0 mmol) was added. This was allowed to stir for 24 h, the resulting white precipitate in the bottom of the flask was filtered away from the solution. The volatiles were removed from the filtrate, leaving a white powder which was washed with toluene (3 × 10 cm$^3$), and the resulting solution was pumped down to half its volume and stored at −25 °C overnight (10 h), resulting in clear block crystals. Yield *ca.* 60%. MS (EI, %): *m*/*z*: 218 ($^t$Bu$_2$GaCl, 42), 183 ($^t$Bu$_2$Ga, 100), 126 ($^t$BuGa, 60), 71 (Ga, 45). IR (cm$^{-1}$): 3476 (O–H stretch, w), 1280 (s), 1164 (m), 1116 (m), 1098 (m), 953 (m), 822 (s), 727 (m). $^1$H NMR: $\delta$ 3.71 [1H, m, *J*(H–H) = 6.11 Hz, CH(CH$_3$)$_2$], 2.12 (1H, s, OH), 1.41 [18H, s, C(C$H_3$)$_3$], 0.86 [6H, d, *J*(H–H) = 6.11 Hz, CH(C$H_3$)$_2$]. $^{13}$C NMR ($CDCl_3$): $\delta$ 67.0 [CH(CH$_3$)$_2$], 31.0 [C(CH$_3$)$_3$], 30.4 [C(CH$_3$)$_3$], 24.9 [CH(CH$_3$)$_2$].

**[Li(HO$^i$Pr)$_4$][($^t$Bu)$_2$GaCl$_2$] (11).** A solution of $GaCl_3$ (1.0 g, 5.7 mmol) in $Et_2O$ (20 cm$^3$) was cooled to −78 °C. To this solution was added $^t$BuLi (6.7 cm$^3$, 1.7 M in pentane, 11.4 mmol), which immediately caused fume evolution upon addition. To the resulting mixture was added isopropanol (10 cm$^3$) as a layer on top of the $Et_2O$ solution. These layers were then cooled to −25 °C, and the two layers slowly mixed over 2 d. The solvent volume was reduced (*ca*. 1 cm$^3$) from which clear crystals were formed. Yield: *ca.* 70%. Mp >200 °C. MS (EI, %): *m*/*z*: 220 ($^t$Bu$_2$GaCl, 5), 183 ($^t$Bu$_2$Ga, 30), 69 (Ga, 18), 57 ($^t$Bu, 100). IR (cm$^{-1}$): 3473 (O–H stretch, w), 1265 (m), 1158 (s), 1096 (m), 1020 (m), 948 (s), 805 (m). $^1$H NMR: $\delta$ 3.80 [6H, septet, *J*(H–H) = 6.15 Hz, CH(CH$_3$)$_2$], 2.62 [6H, s, OH], 1.56 [18 H, s, C(C$H_3$)$_3$], 1.01 [36H, d, *J*(H–H) = 6.15 Hz, CH(C$H_3$)$_2$]. $^{13}$C NMR: $\delta$ 65.6 [CH(CH$_3$)$_2$], 30.5 [C(CH$_3$)$_3$], 27.7 [C(CH$_3$)$_3$], 25.2 [CH(CH$_3$)$_2$].

## Crystallographic studies

Crystals of compounds **1**–**6**, and **8**–**11** were sealed in glass capillaries under argon. Crystal and data collection and solution details are given in Table 7. Standard procedures in our laboratory have been described previously.[6] Data were collected on either a Rigaku AFC-5S serial diffractometer or a Bruker CCD SMART system, equipped with graphite monochromated Mo-Kα radiation ($\lambda$ = 0.71073 Å) and corrected for Lorentz and polarization effects. The structures were solved using the direct methods program XS[51] and difference Fourier maps and refined by using full matrix least squares method.

Disorder and/or high thermal motion were noted in most of the compounds, usually associated with the *tert*-butyl groups. Of particular note were the observations of two positions each for the fluorine atoms in compound **3** (in a 1 : 1 ratio) and two positions each for the methyl carbons [C(16)–C(18)] of a *tert*-butyl group in compound **5** (in a 1 : 1 ratio), and the isopropyl groups in compound **10** were disordered over all three possible sites (each one being refined as two-thirds carbon and one-third hydrogen). In addition, the room temperature data for compounds **1** and **11** was particularly bad, leading to high thermal motion and poor resolution. Due to low crystal quality and a resultant paucity of data, the refinements for compounds **1**, **4** and **11** lack sufficient precision to allow detailed discussion. However, connectivity and other broad structural features are undoubtedly correct.

All non-hydrogen atoms were refined with anisotropic thermal

**Table 7** Summary of X-ray diffraction data

| Compound | [($^t$Bu)$_2$Ga{μ-OCH(CF$_3$)$_2$}]$_2$ (**1**) | [($^t$Bu)$_2$Ga(μ-O$_2$CEt)]$_2$ (**2**) | [($^t$Bu)$_2$Ga(μ-O$_2$CCF$_3$)]$_2$ (**3**) | [($^t$Bu)$_2$Ga{μ-OC(Ph)N(H)}]$_2$ (**4**) | [($^t$Bu)$_2$Ga{μ-OC(Me)NPh}]$_2$ (**5**) | ($^t$Bu)$_3$Ga[OC(Ph)NMe$_2$] (**6**) | ($^t$Bu)$_2$Ga[ON(H)C(O)Ph] (**8**) | [($^t$Bu)$_2$Ga(μ-O$_2$S(CF$_3$)O)]$_2$ (**9**) | ($^t$Bu)$_2$Ga(μ-Cl)$_2$Li($^t$HOPr)$_2$ (**10**) | [Li($^t$HOPr)$_4$][($^t$Bu)$_2$GaCl$_2$] (**11**) |
|---|---|---|---|---|---|---|---|---|---|---|
| Formula | $C_{22}H_{38}F_{12}Ga_2O_2$ | $C_{22}H_{46}Ga_2O_4$ | $C_{20}H_{36}F_6Ga_2O_4$ | $C_{30}H_{48}Ga_2N_2O_2$ | $C_{32}H_{52}Ga_2N_2O_2$ | $C_{21}H_{38}GaNO$ | $C_{15}H_{24}GaNO_2$ | $C_{18}H_{36}F_6Ga_2O_6S_2$ | $C_{14}H_{32}Cl_2GaLiO_2$ | $C_{28}H_{60}Cl_2GaLiO_4$ |
| $M_w$ | 701.969 | 514.051 | 593.940 | 608.169 | 636.223 | 390.262 | 320.084 | 666.049 | 379.976 | 502.184 |
| Crystal system | Monoclinic | Monoclinic | Triclinic | Triclinic | Triclinic | Monoclinic | Monoclinic | Triclinic | Triclinic | Orthorhombic |
| Space group | *C*2 | *C*2/*c* | *P*$\bar{1}$ | *P*$\bar{1}$ | *P*$\bar{1}$ | $P2_1/n$ | $P2_1/n$ | *P*$\bar{1}$ | *P*$\bar{1}$ | $P2_12_12_1$ |
| *a*/Å | 17.112(3) | 23.809(5) | 9.097(2) | 11.911(1) | 9.159(2) | 10.300(2) | 16.845(3) | 8.753(2) | 11.860(2) | 20.951(4) |
| *b*/Å | 11.240(2) | 8.621(2) | 10.384(2) | 16.703(3) | 12.252(3) | 14.990(3) | 12.449(3) | 9.297(2) | 11.878(2) | 16.287(3) |
| *c*/Å | 9.015(2) | 16.406(3) | 8.752(2) | 8.372(2) | 8.514(2) | 30.720(6) | 16.953(3) | 10.645(2) | 9.417(2) | 9.470(2) |
| *α*/° | | | 100.46(3) | 92.84(3) | 102.14(3) | | | 92.07(3) | 112.15(3) | |
| *β*/° | 120.73(3) | 122.64(3) | 113.59(3) | 103.61(3) | 112.37(3) | 93.39(3) | 94.47(3) | 101.53(3) | 94.09(3) | |
| *γ*/° | | | 94.08(3) | 93.11(3) | 78.59(3) | | | 114.86(3) | 92.74(3) | |
| *V*/Å$^3$ | 1490.5(5) | 2835(1) | 735.5(3) | 1613.1(6) | 856.4(3) | 4735(2) | 3544(1) | 763.0(3) | 1221.6(4) | 3231(1) |
| *Z* | 2 | 4 | 1 | 2 | 1 | 8 | 8 | 1 | 2 | 4 |
| *μ*/cm$^{-1}$ | 1.90 | 1.02 | 1.89 | 1.70 | 1.600 | 1.17 | 1.55 | 1.97 | 1.34 | 1.034 |
| *T*/K | 298 | 298 | 298 | 298 | 298 | 298 | 298 | 298 | 298 | 298 |
| Reflections collected | 2071 | 1910 | 2073 | 3120 | 2402 | 20955 | 3628 | 2133 | 3404 | 2416 |
| independent | 1039 | 1858 | 1925 | 2924 | 2233 | 6764 | 3442 | 2001 | 3223 | 2416 |
| observed ($\|F_o\| > 4.0\sigma\|F_o\|$) | 949 | 1326 | 1491 | 1507 | 1845 | 4103 | 2370 | 1767 | 2331 | 1347 |
| *R* | 0.115 | 0.0554 | 0.0516 | 0.102 | 0.042 | 0.075 | 0.086 | 0.054 | 0.117 | 0.075 |
| $R_w$ | 0.121 | 0.141 | 0.132 | 0.252 | 0.114 | 0.208 | 0.229 | 0.144 | 0.076 | 0.198 |

parameters in compounds **2**–**5** and **8**–**10**. Due to problems of unresolvable disorder, the methyl groups of three *tert*-butyls were refined isotropically in compound **6**. Due to lack and poor quality of data only the Ga atoms in compound **1** and the Ga, Cl and O atoms in **11** were refined anisotropically. All the hydrogen atoms were placed in calculated positions [$U_{iso} = 0.08$; $d$(C–H) = 0.96 Å] for refinement. Neutral-atom scattering factors were taken from the usual source.[52] Refinement of positional and anisotropic thermal parameters led to convergence (see Table 7).

CCDC reference number 186/1771.

## Acknowledgements

Financial support for this work is provided by the Robert A. Welch Foundation and the Office of Naval Research. The Bruker CCD Smart System Diffractometer was funded by the Robert A. Welch Foundation and the Bruker Avance 200 NMR spectrometer was purchased with funds from ONR Grant N00014-96-1-1146. A. R. B. acknowledges the support of the Alexander von Humboldt Foundation for a Senior Scientist Fellowship and Professor H. W. Roesky for his support, hospitality and useful scientific discussion.

## References

1 For review articles, see, (*a*) A. R. Barron, *Chem. Soc. Rev.*, 1993, 93; (*b*) A. R. Barron, *Comments Inorg. Chem.*, 1993, **14**, 123; (*c*) A. R. Barron, *Macromol. Symp.*, 1995, **97**, 15; (*d*) A. R. Barron, *Adv. Mater. Optics Electron.*, 1995, **5**, 245.
2 C. A. Tolman, *Chem. Rev.*, 1977, **77**, 313.
3 (*a*) E. A. Jeffery, T. Mole and J. K. Saunders, *Aust. J. Chem.*, 1968, **21**, 137; (*b*) E. A. Jeffery, T. Mole and J. K. Saunders, *Aust. J. Chem.*, 1968, **21**, 649.
4 (*a*) H.-U. Schwering, E. Jungk and J. Weidlein, *J. Organomet. Chem.*, 1975, **91**, C4; (*b*) W. M. Cleaver and A. R. Barron, *Chemtronics*, 1989, **4**, 146.
5 E. G. Gillan, S. G. Bott and A. R. Barron, *Chem. Mater.*, 1997, **9**, 796.
6 M. R. Mason, J. M. Smith, S. G. Bott and A. R. Barron, *J. Am. Chem. Soc.*, 1993, **115**, 4971.
7 C. J. Harlan, M. R. Mason and A. R. Barron, *Organometallics*, 1994, **13**, 2957.
8 C. J. Willis, *Coord. Chem. Rev.*, 1988, **88**, 133 and references therein.
9 D. G. Tuck, *Comprehensive Organometallic Chemistry*, ed. G. Wilkinson, F. G. A. Stone and E. W. Abel, Pergamon Press, Oxford, 1982, vol. 1, ch. 7.
10 *Handbook of Chemistry and Physics*, 60th edn., CRC Press, Boca Raton, FL, 1980, D-194.
11 T. J. Barbarich, C. D. Rithner, S. M. Miller, O. P. Anderson and S. H. Strauss, *J. Am. Chem. Soc.*, 1999, **121**, 4289 and references therein.
12 W. M. Cleaver, A. R. Barron, A. R. McGufey and S. G. Bott, *Polyhedron*, 1994, **13**, 2831.
13 H. D. Hausen, K. Sille, J. Weidlein and W. Schwartz, *J. Organomet. Chem.*, 1978, **160**, 411.
14 A. Keys, S. G. Bott and A. R. Barron, *Polyhedron*, 1998, **17**, 3121.
15 (*a*) J. J. Eisch, in *Comprehensive Organometallic Chemistry*, ed. G. Wilkinson, F. G. A. Stone and E. W. Abel, Pergamon Press, Oxford, 1988, vol. 1, ch. 6; (*b*) J. Weidlein, *Z. Anorg. Allg. Chem.*, 1970, **378**, 245; (*c*) A. Pietrzykowski, S. Pasynkiewicz and J. Poplawska, *Main Group Metal Chem.*, 1996, **18**, 651; (*d*) G. V. Zenina, N. I. Sheverdina and K. A. Kocheskov, *Dokl. Chem.* (*Engl. Transl.*), 1970, **195**, 786.
16 H. D. Hausen, K. Sille, J. Weidlein and W. Schwarz, *J. Organomet. Chem.*, 1978, **160**, 411.
17 M. J. Zaworotko, R. D. Rogers and J. L. Atwood, *Organometallics*, 1982, **1**, 1179.
18 Gallium: Organometallic Chemistry. A. R. Barron and M. B. Power, *Encyclopedia of Inorganic Chemistry*, ed. R. Wells, Wiley, New York, 1995.
19 C. C. Landry, A. Hynes, A. R. Barron, I. Haiduc and C. Silvestru, *Polyhedron*, 1996, **15**, 391.
20 R. Kumar, V. S. J. de Mel and J. P. Oliver, *Organometallics*, 1989, **8**, 2488.
21 M. B. Power, S. G. Bott, D. L. Clark, J. L. Atwood and A. R. Barron, *Organometallics*, 1990, **9**, 3086.

22 A. Zwierzak and I. Podstawczynska, *Angew. Chem.*, *Int. Ed. Engl.*, 1977, **16**, 703.
23 C. N. McMahon, S. G. Bott and A. R. Barron, *J. Chem. Soc.*, *Dalton Trans.*, 1997, 3129.
24 R. Taylor and O. Kennard, *Acc. Chem. Res.*, 1984, **17**, 320.
25 G. A. Olah, O. Farooq, S. M. F. Farnia and J. A. Olah, *J. Am. Chem. Soc.*, 1988, **110**, 2560.
26 S. Kobayashi, K. Koide and M. Ohno, *Tetrahedron Lett.*, 1990, **31**, 2435.
27 A. H. Cowley, F. P. Gabbaï, D. A. Atwood, C. J. Carrano, L. M. Mokry and M. R. Bond, *J. Am. Chem. Soc.*, 1994, **116**, 1559.
28 A. Keys, S. G. Bott and A. R. Barron, *Chem. Commun.*, 1996, 2339.
29 C. C. Landry, A. Hynes, A. R. Barron, I. Haiduc and C. Silvestru, *Polyhedron*, 1996, **15**, 391.
30 F. E. Hahn and B. Schneider, *Z. Naturforsch.*, *Teil B*, 1990, **45**, 134.
31 See for example, E. G. Gillan, S. G. Bott and A. R. Barron, *Chem. Mater.*, 1997, **9**, 796 and references therein.
32 J. L. Atwood, S. G. Bott, P. B. Hitchcock, C. Eaborn, R. S. Shariffudin, J. D. Smith and A. C. Sullivan, *J. Chem. Soc.*, *Dalton Trans.*, 1987, 747.
33 M. A. Petrie, P. P. Power, H. V. R. Dias, K. Ruhlandt-Senge, K. M. Waggoner and R. J. Wehmschulte, *Organometallics*, 1993, **12**, 1086.
34 A. M. Arif, A. H. Cowley, T. M. Elkins and R. A. Jones, *J. Chem. Soc.*, *Chem. Commun.*, 1986, 1776.
35 A. Keys, S. G. Bott and A. R. Barron, *Chem. Mater.*, 1999, **11**, 3578.
36 S. L. Stoll, S. G. Bott and A. R. Barron, *J. Chem. Soc.*, *Dalton Trans.*, 1997, 1315.
37 C. L. Aitken and A. R. Barron, *J. Chem. Cryst.*, 1996, **26**, 293.
38 J. T. Leman and A. R. Barron, *Organometallics*, 1989, **8**, 2214.
39 S. U. Ghazi, M. J. Heeg and J. P. Oliver, *Inorg. Chem.*, 1994, **33**, 4517.
40 J. A. Zerkowski, J. C. MacDonald and G. M. Whitesides, *Chem. Mater.*, 1994, **6**, 1250.
41 H. D. Hausen, H. J. Guder and W. Schwartz, *J. Organomet. Chem.*, 1977, **132**, 37.
42 Y. Koide, J. A. Francis, S. G. Bott and A. R. Barron, *Polyhedron*, 1998, **17**, 983.
43 O. T. Beachley, Jr., M. R. Churchill, J. C. Pazik and J. W. Ziller, *Organometallics*, 1987, **6**, 2088.
44 M. B. Power, W. M. Cleaver, A. W. Apblett, A. R. Barron and J. W. Ziller, *Polyhedron*, 1992, **11**, 477.
45 F. Schwan, S. P. Mallela and R. A. Geanangel, *J. Chem. Soc.*, *Dalton Trans.*, 1996, 4183.
46 G. Linti, R. Frey, W. Köstler and H. Urban, *Chem. Ber.*, 1996, **129**, 561.
47 C. E. Bethley, C. L. Aitken, Y. Koide, C. J. Harlan, S. G. Bott and A. R. Barron, *Organometallics*, 1997, **16**, 329.
48 See (*a*) I. Haiduc, *The Chemistry of Inorganic Ring Systems*, Wiley, Chichester, 1970, vol. II, ch. 7, p. 1018; (*b*) M. Cesari and S. Cucinella, in *The Chemistry of Inorganic Homo- and Heterocycles*, ed. I. Haiduc and D. B. Sowerly, Academic Press, New York, 1987, vol. 2, p. 167; (*c*) J. P. Oliver, R. Kumar and M. Taghiof, in *Coordination Chemistry of Aluminum*, ed. G. H. Robinson, VCH, New York, 1993, ch. 5, p. 167; (*d*) H. D. Hausen, F. Gerstner and W. Schwarz, *J. Organomet. Chem.*, 1978, **145**, 277.
49 R. A. Kovar, H. Derr, D. Brandau and J. O. Callaway, *Inorg. Chem.*, 1975, **14**, 2809.
50 A. Zwierzak and I. Podstawczynska, *Angew. Chem.*, *Int. Ed. Engl.*, 1977, **16**, 702.
51 Nicolet Instruments Corporation, Madison, WI, USA, 1988.
52 *International Tables for X-Ray Crystallography*, Kynoch Press, Birmingham, 1974, vol. 4.

*Paper a905281j*